

University of Windsor

Scholarship at UWindor

Electronic Theses and Dissertations

Theses, Dissertations, and Major Papers

2022

Patterns and Behaviours of Barrier Breaching in Lacustrine Environments: A Case Study from the Point Pelee Foreland

Jenny Gharib
University of Windsor

Follow this and additional works at: <https://scholar.uwindsor.ca/etd>



Part of the [Environmental Sciences Commons](#)

Recommended Citation

Gharib, Jenny, "Patterns and Behaviours of Barrier Breaching in Lacustrine Environments: A Case Study from the Point Pelee Foreland" (2022). *Electronic Theses and Dissertations*. 8931.
<https://scholar.uwindsor.ca/etd/8931>

This online database contains the full-text of PhD dissertations and Masters' theses of University of Windsor students from 1954 forward. These documents are made available for personal study and research purposes only, in accordance with the Canadian Copyright Act and the Creative Commons license—CC BY-NC-ND (Attribution, Non-Commercial, No Derivative Works). Under this license, works must always be attributed to the copyright holder (original author), cannot be used for any commercial purposes, and may not be altered. Any other use would require the permission of the copyright holder. Students may inquire about withdrawing their dissertation and/or thesis from this database. For additional inquiries, please contact the repository administrator via email (scholarship@uwindsor.ca) or by telephone at 519-253-3000ext. 3208.

**Patterns and Behaviours of Barrier Breaching
in Lacustrine Environments: A Case Study
from the Point Pelee Foreland**

By

Jenny Gharib

A Thesis

Submitted to the Faculty of Graduate Studies
through the School of the Environment
in Partial Fulfillment of the Requirements for
the Degree of Master of Science
at the University of Windsor

Windsor, Ontario, Canada

© 2022, Jenny Gharib

**Patterns and Behaviours of Barrier Breaching
in Lacustrine Environments: A Case Study
from the Point Pelee Foreland**

by

Jenny Gharib

APPROVED BY:

P. Wernette

United States Geological Survey

C. Proctor

School of the Environment

C. Houser, Advisor

School of the Environment

August 26th, 2022

Declaration of Co-Authorship / Previous Publication

I. Co-Authorship

I hereby declare that this thesis incorporates material that is result of joint research, as follows:

Chapter 6 of the thesis includes the outcome of publications which have the following other co-authors: Alex Smith and Chris Houser. In all cases only my primary contributions towards these publications are included in this thesis; Alex Smith contributed to experimentation, analysis, writing, and editing the manuscript; and Chris Houser contributed feedback on the refinement of ideas.

I am aware of the University of Windsor Senate Policy on Authorship and I certify that I have properly acknowledged the contribution of other researchers to my thesis, and have obtained written permission from each of the co-authors to include the above materials in my thesis.

I certify that, with the above qualification, this thesis, and the research to which it refers, is the product of my own work.

II. Previous Publication

This thesis includes one original paper that has been previously published, as follows:

Thesis Chapter	Publication title/full citation	Publication status*
Chapter 6	Gharib, J., Smith, A. & Houser, C. (2021) Barrier beaches and breaches: Historical changes on the Point Pelee Foreland. <i>Journal of Great Lakes Research</i> . [Online] 47 (6), 1554–1564. Available from: doi:10.1016/j.jglr.2021.06.011.	Published

I certify that I have obtained a written permission from the copyright owners to include the above published materials in my thesis. I certify that the above material describes work completed during my registration as a graduate student at the University of Windsor.

III. General

I declare that, to the best of my knowledge, my thesis does not infringe upon anyone's copyright nor violate any proprietary rights and that any ideas, techniques, quotations, or any other material from the work of other people included in my thesis, published or otherwise, are fully acknowledged in accordance with the standard referencing practices. Furthermore, to the extent that I have included copyrighted material that surpasses the bounds of fair dealing within the meaning of the Canada Copyright Act, I certify that I have obtained a written permission from the copyright owners to include such materials in my thesis.

I declare that this is a true copy of my thesis, including any final revisions, as approved by my thesis committee and the Graduate Studies office, and that this thesis has not been submitted for a higher degree to any other University or Institution.

Abstract

The Great Lakes are non-tidal, but experience significant water level fluctuations at hourly, seasonal, and decadal scales. In response to elevated water levels, barrier beach-ridges, including those located on the eastern shore of the Point Pelee foreland, experience accelerated erosion, overwash, and breaching leading to the removal or burial of vegetation, and damage to infrastructure and vulnerable habitat. Historical aerial imagery between 1931–2022 and annual average lake levels between 1920–2022 were examined to characterize barrier retreat and breach initiation, expansion, and closure. The timing and rate of transgression and progradation, overwash, and breaching are dependent on decadal-scale variations in water level. Ephemeral breaches and deposits were found to be a significant source of sediment transported landwards, this may represent a self-reinforcing cycle that promotes breach fill-in processes, even during high lake levels, and increases the barrier width and resiliency in response to further lake level fluctuations. This self-reinforcing cycle is disrupted by modified shorelines that limit sediment supply, leading to a persistent opening that can only close if water levels drop significantly, or new sediment is added to the system. Barrier breaching is a natural process in lacustrine systems with water level fluctuations, but the process is interrupted by shoreline modifications, putting critical ecosystems at risk.

Acknowledgements

I would like to express my appreciation to my supervisor, Chris Houser, for his support during the completion of this project, and to my committee, Cameron Proctor and Phil Wernette, for their valuable feedback. I would also like to express my gratitude to the Windsor Coastal Group for their advice and support throughout the data collection process and writing process, and to the staff at Point Pelee National Park and Essex Region Conservation Authority for permitting and supporting this work.

My deepest appreciation goes to my parents, my brothers, my boyfriend, and my friends, who helped keep me motivated and in good spirits.

Table of Contents

Declaration of Co-Authorship / Previous Publication	iii
Abstract	v
Acknowledgements	vi
1. Introduction	1
2. Background and Literature Review	6
2.1 Barrier Beaches	6
2.2 Barrier Behaviour	6
2.3 Geological Influence on Barriers	10
2.3.1 Basement Slope	10
2.3.2 Basement Topography, Erodibility, and Shoreface Morphology	11
2.3.3 Sediment Supply	14
2.4 Barrier Breaching	15
2.5 Elevated Water Levels	21
2.6 Lake Ice Coverage	22
2.6.1 Under-Ice Currents	24
2.6.2 Ice Scouring	24
2.7 Barrier Breach Examples	25
2.8 Variations in Fish Species Composition due to Breach Events	27
3. Purpose and Objectives	28
3.1 Chapter One: Historical Changes on the Point Pelee Foreland	28
3.2 Chapter Two: Breaching Patterns at Hillman Beach and East Beach	28
4. Study Site	29

5. Methodology	34
6. Historical Changes on the Point Pelee Foreland	39
6.1 Results	39
6.1.1 Hillman Beach barrier (1973-2020)	39
6.1.2 East Beach barrier (1931-2019)	42
6.1.3 Breach initiation, expansion, and closure (2016-2020)	45
6.2 Discussion	48
6.3 Conclusion	53
7. Breach Recovery at Hillman Beach and East Beach	54
7.1 Results	54
7.1.1 East Beach (EB)	55
7.1.2 Hillman Beach (HB)	59
7.2 Discussion	63
7.3 Conclusion on Breach Recovery	70
8. Conclusion and Future Research	72
References	74
Appendix	81
Vita Auctoris	87

1. Introduction

Coastal systems in the Laurentian Great Lakes of North America (Figure 1), as with other lacustrine environments, are highly sensitive to variations in lake levels that can vary significantly in magnitude and occur over multiple temporal scales. Hourly variability occurs through wind set-up and can reach upwards of 2 m during storm events, seasonal variability can vary between 0.2 – 0.4 m in response to the balance of precipitation, snowmelt, and evaporation, and interannual variability can range up to 2 m and is controlled by longer-term patterns in precipitation and temperature (Quinn, 2002). Although water levels in the Great Lakes have gone through many fluctuations, in recent years there have been record highs since the earliest recorded data from 1918. Lake Erie, specifically, has low-lying shorelines and shallow depths, resulting in large response to meteorological events and increased shoreline flooding and erosion during periods of high water level (Hamblin, 1987).

Storm surge, an abnormal, sudden rise of lake level during a storm, causes the most destruction during a storm event. High water levels cause flooding that brings the coast inland, and pounding waves erode large sections of the coastline (Danard, 2003). This storm-based flooding and erosion can also occur during meteotsunamis, of which are common in the Great Lakes, especially Lake Erie, which notably has a relatively shallow and uniform depth (Angove et al., 2021). Following storm surge and meteotsunamis, a setdown, or decreased water levels, takes place on the opposite side of the lake, leading to back-and-forth oscillations of water level (i.e. seiche) (Sogut et al., 2018). The seiche periods of Lake Erie are the longest of any of the Great Lakes, and also have the largest amplitudes (Hamblin, 1987).

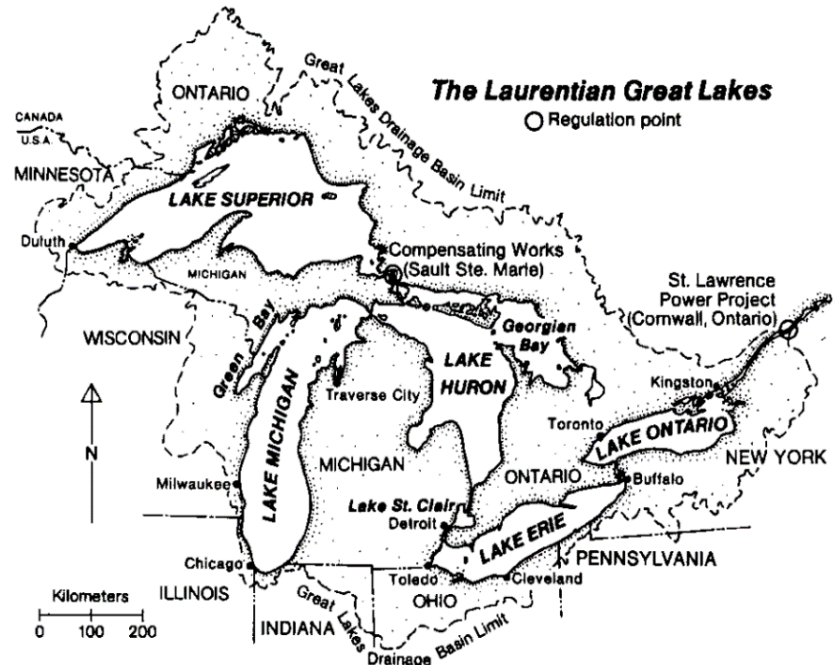


Figure 1: The Laurentian Great Lakes; Lake Superior, Lake Michigan, Lake Huron, Lake Erie, and Lake Ontario (Quinn, 2002).



Figure 2: Barrier breaching at East Beach, facing south, located on the eastern shoreline of Point Pelee National Park, in Ontario, Canada.

A barrier beach is a narrow, short, shore-parallel beach that is separated from the mainland by a lagoon, marsh, or estuary (Otvos, 2012). Water level fluctuations modify barriers on the Great Lakes through shoreline change rates (BaMasoud and Byrne, 2011), breaching and overwash (Davidson-Arnott and Fisher, 1992), modifying fetch lengths and aeolian transport (Davidson-Arnott and Law, 1996), and sandwave migration (Davidson-Arnott and Van Heyningen, 2003). Increases in water levels can also affect backbarrier marsh ecosystems through burial by overwash and exposure to flooding and wave activity following breaching (Herdendorf, 1987, Keough et al., 1999). With a changing climate, the Great Lakes are projected to experience increased water temperatures, alteration of water chemistry, oxygen depletion, and released nutrients and minerals from lake sediments (Hartmann, 1990), making the role of barrier beaches increasingly significant in the protection of sensitive ecosystems and habitats.

The resiliency of a barrier depends on its ability to recover in elevation and vegetation coverage prior to the next event (Houser et al., 2018). The elevation of a barrier controls overwash and inundation (Sallenger, 2000) that can subsequently lead to breaching. Breaching, controlled by long-term lake level cycles, leads to landward transgression of the shoreline (Davidson-Arnott & Reid, 1994). Storm generated inlets, often developing during high lake level periods, can act as a conduit for landward sediment transport that increases the width and height of the barrier (Mattheus et al., 2016). Barrier breaching (Figure 2) can occur during periods of high-water levels and storm surges when water level exceeds a critical elevation relative to the barrier crest (Kraus, 2003) and scours a trough between the water bodies on both sides. Alternatively, a narrow barrier breach can allow for high water levels to seep through porous sediment, liquify it, and allow the sediment to be quickly transported offshore (Kraus et al., 2002). Breach events can induce considerable variation in species composition that will in turn introduce predators and competitors,

introducing or extirpating native species. As of 2022, 15 breached barriers are located across the Great Lakes at various stages of opening and recovery (Table 1).

Table 1: Barrier breaching across the Great Lakes, most commonly found at Lake Erie and Lake Ontario.

Barrier	Lake
East Beach, Point Pelee National Park, ON	Lake Erie
Hillman Beach, Hillman Marsh Conservation Area, ON	Lake Erie
Conneaut Beach, Conneaut, OH	Lake Erie
Elk Creek, Erie County, PA	Lake Erie
Talbot Creek, Elgin County, ON	Lake Erie
Tyrconnell Beach, Tyrconnell, ON	Lake Erie
North Bar Beach, Empire Township, MI	Lake Michigan
Petobego Beach, Grand Traverse County, MI	Lake Michigan
Ajax Waterfront, Ajax, ON	Lake Ontario
Lynde Creek, Durham, ON	Lake Ontario
Petticoat Creek, Pickering, ON	Lake Ontario
Turtle/Sheridan Creek, Mississauga, ON	Lake Ontario
Wild Beach, Whitby, ON	Lake Ontario
Terrace Bay Beach, Thunder Bay District, ON	Lake Superior
Lightfoot Bay, Skanee, MI	Lake Superior

High Annual Maximum Ice Coverage (AMIC) is an important control on lacustrine breaching as lake ice protects shorelines from the impact of winter storms. Lake Erie’s AMIC is skewed to higher values due to the relatively shallow depth of the lake, however, the winter of

2019/2020 had a record low maximum ice cover of 15% (Gharib et al., 2021; Assel et al., 2003) (Figure 3). Between 2013 and 2020, the level of Lake Erie rose by 0.83 m, with water levels reaching the previously recorded average monthly water level high of 175.04 m set in 1986, surpassing it at 175.14 m in 2019, and again at 175.1 m in 2020. During this time, barrier beaches located on the eastern shore of the Point Pelee foreland experienced accelerated rates of erosion, breaching, loss of vegetation, and damage to infrastructure. Barrier breaching exposes the lagoon to harsh waves from the open water, jeopardizing the stability of sensitive ecosystems and habitats, and can raise the water level in the lagoon, subsequently leading to flooding of the mainland. Climate change in the Great Lakes is projected to increase the variability of water level fluctuations, further intensifying these effects.

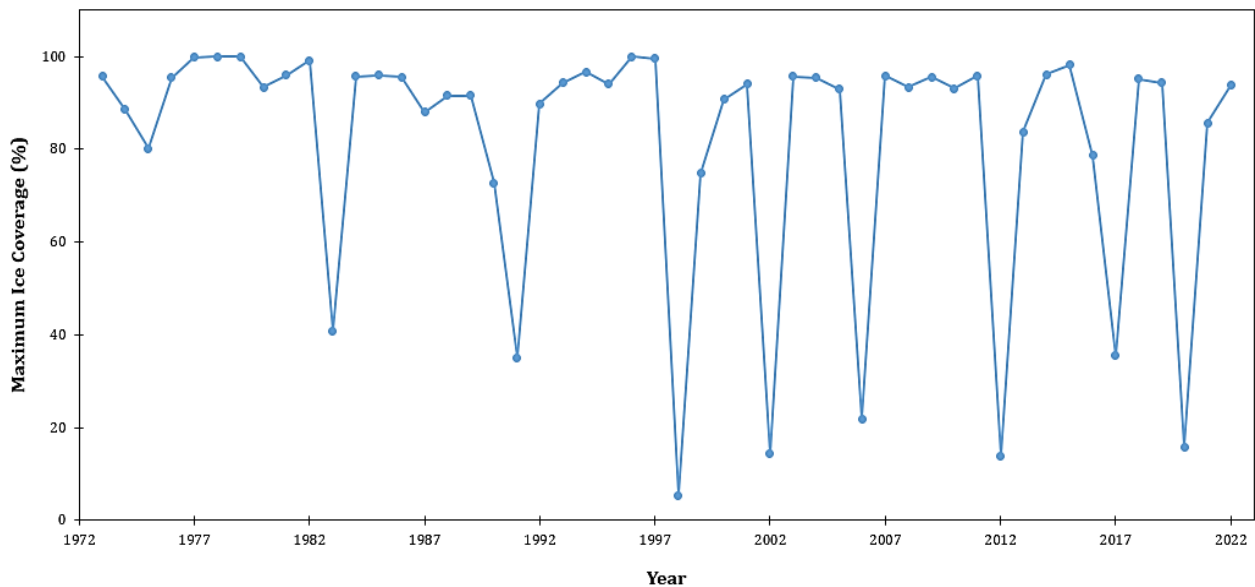


Figure 3: Lake Erie's Historical Annual Maximum Ice Coverage (AMIC) from 1976 to 2020.

2. Background and Literature Review

2.1 Barrier Beaches

Barrier beaches vary in height, width, composition (gravel/sand), orientation and exposure to wave processes and extreme storm events (Orford, 1995). They respond to various drivers; short-term (low magnitude/high frequency wave processes), episodic (wave energy and water level variations during storms), medium term (cumulative effect of waves and climate oscillations), or long-term (sea-level change) (Cooper et.al, 2018; Houser et al., 2008). These drivers, despite constantly changing, are mediated by non-dynamic variables such as variations including basement slope, basement topography and erodibility, external sediment supply, coastal orientation, shoreline lithification, and shoreface morphology (Cooper et al., 2018). Barrier beach and island morphology is the product of these modern processes interacting with pre-existing topography and bathymetry (Wernette et al., 2018). Understanding barrier behaviour at various time scales and how it will adapt to sea level rise is crucial due to increased human development either on, or adjacent to, barrier systems. Barriers possess essential protective services to inshore environments including the dissipation of wave energy inshore, imposing a sharp contrast in nearshore and inshore sediment types, protection against storm destruction, protection for inshore ecological habitats, and maintain continuous path of littoral drift in sediment transmission (Otvos, 2012). The six main components of a barrier/ lagoon system are the mainland, backbarrier lagoon, inlet, barrier island, barrier platform, and shoreface (Figure 4) (Cooper et al., 2018).

2.2 Barrier Behaviour

Cooper et al. (2018) proposes four behavioural categories for the response of barrier: rollover, erosion, overstepping and aggradation/progradation (Figure 5). The rollover model shows

barrier behaviour as being dominated by overwash as a response to storm events. Sediment volume is maintained during overwash events, but the barrier migrates landward. This model is highly observed and reported, specifically by Hosier & Cleary (1977) at Masonboro Island on the southeastern shore of Northern Carolina, where the island has seen approximately 61 m of retreat in the last 30 years. Migration rate has been linked to 1) frequency of overwashing storms, 2) barrier volume, 3) the gradient of the surface where the barrier is migrating, and 4) the rate of sea level rise (Cooper et al., 2018).

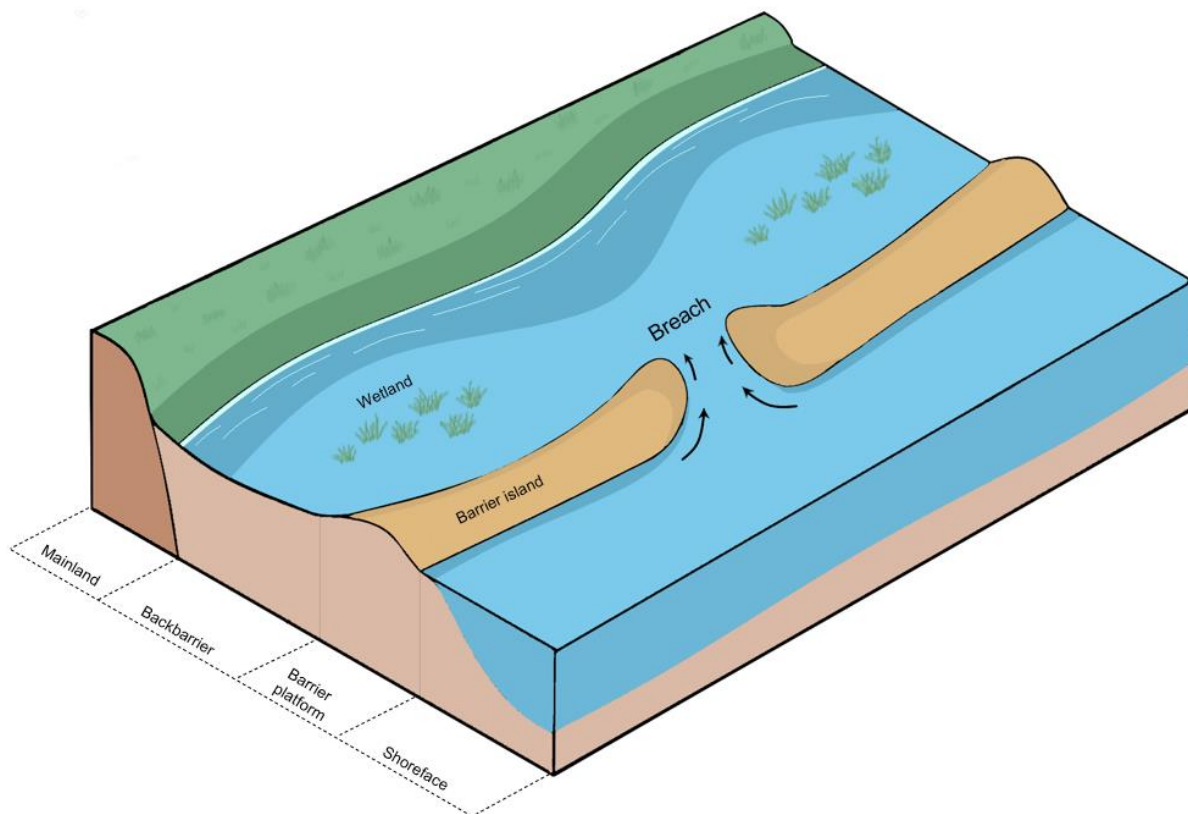


Figure 4: The six main components of a barrier system: the mainland, the backbarrier, the barrier platform, the barrier island, the shoreface, and the inlet.

The erosional response involves the seaward loss of sediment during transgression. This is best seen through the Bruun Rule (Carter, 1988), where a barrier experiences dune, surf zone, and

shoreface retreat simultaneously, however it is not widely observed as the shoreface often retreats slower. Overstepping occurs when a barrier is drowned in situ, leaving its sediments on the seabed. This involves a fast rate of sea level rise accompanied by slow reaction time of a barrier. In the early stages of overstepping, barrier breaching is common when water levels exceed the elevation of the barrier before it is completely drowned. During overstepping, barrier preservation is reliant on sediment cementation, long relaxation times, back barrier accommodation, large barrier sediment volume, and low wave energy (Cooper et al., 2018; Orford et al., 1995). Lastly, barrier progradation or aggradation can occur in either falling or rising sea level conditions if the sediment supply is high enough. Most sediment rich barriers exhibit combinations of both aeolian and wave deposits (Cooper et al., 2018).

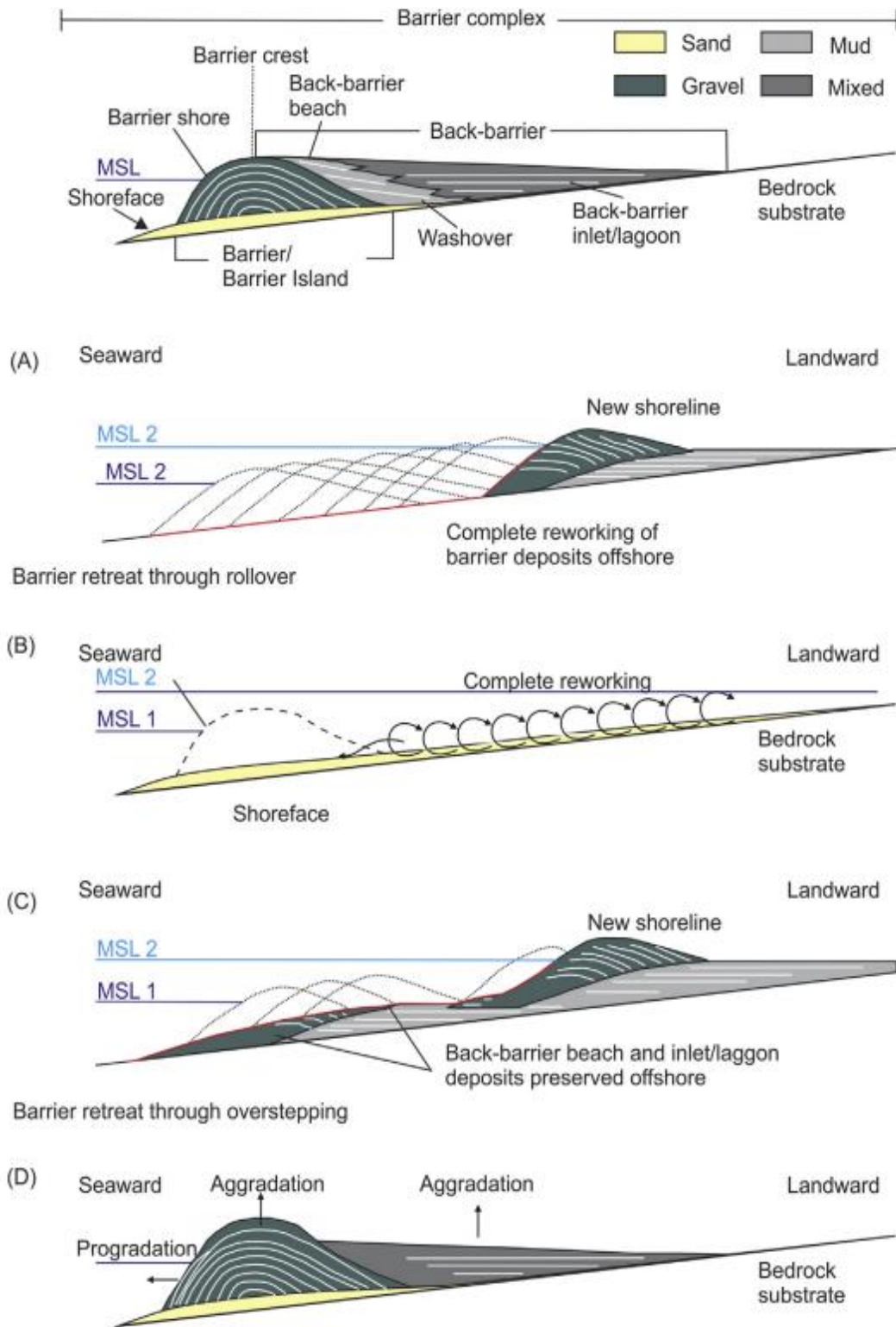


Figure 5: Profile models of barrier response. (A) Rollover; (B) Erosion; (C) Overstepping; (D) Progradation/aggradation (from Cooper et al., 2018).

2.3 Geological Influence on Barriers

The initial morphology of a barrier sets limits to the processes that may occur including overwash, dune building, longshore drift, and inlet-associated processes. These pre-modern features modify wave and current processes, subsequently controlling patterns of sediment erosion, transport, and deposition (Houser, 2012). Cooper et al. (2018) creates a hierarchy of geological parameters, identifying the primary geological controls as basement characteristics (slope, topography, and erodibility), shoreface morphology, sediment supply and lithification. These will subsequently influence secondary controls such as barrier orientation, extent, volume, and morphology. These features are all determining factors in the possibility of overwash occurrence, inlet formation, barrier retreat, and shoreline erosion.

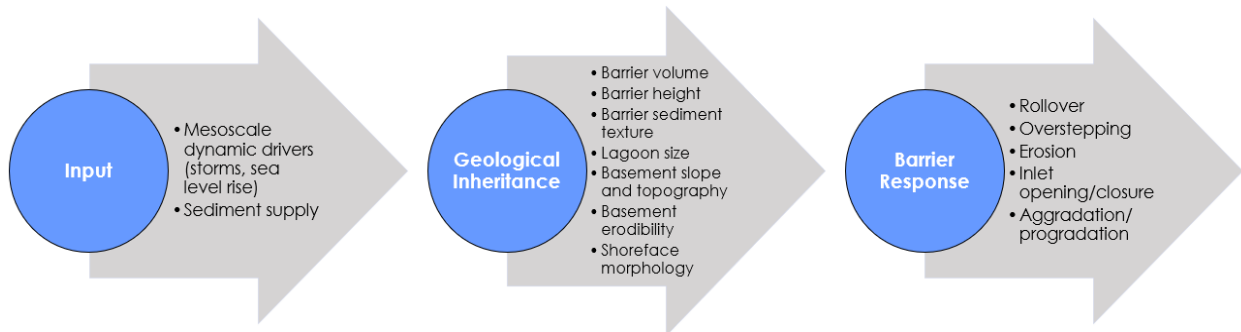


Figure 6: Linkage between energy and sediment output, geological inheritance and constraints, and subsequent barrier response. Adapted from Cooper et al., (2018).

2.3.1 Basement Slope

Studies have shown that the basement slope of a barrier controls the accommodation space available for migration and influences whether rollover, drowning, erosion, or accretion occurs. Steeper basement slopes have been found to cause landward transgression at a faster rate than flatter surfaces (Schwab et al., 2000). Steeper slopes also promote the offshore movement of sandy sediment, where flatter slopes promoted onshore movement. This, in turn, causes barriers with

steeper slopes to remain stable and adapt during sea-level rise as the onshore and offshore movement of sediment creates an equilibrium. However, steeper slopes have also been documented to more effectively focus shoreface erosion, with a greater amount of erosion per unit time (Cooper et al., 2018). Brenner et al. (2015) conducted a study on Metompkin Island, Virginia, and found that rather than just basement slope, a wide back barrier is one of the most important variables to affect barrier migration, where a wide back barrier would result in rollover, rather than in place drowning or erosion.

2.3.2 Basement Topography, Erodibility, and Shoreface Morphology

Topographic highs and lows significantly influence the behaviour and morphology of barriers and backbarriers. Headlands projecting out from the coastline act as anchor points that help fix the position of barriers during sea level rise, while also acting as a source of sediment (Orford et al., 2002). Barriers migrate landwards over unerodable bedrock (due to overwash and aeolian processes) encountering areas of low and high bedrock that subsequently determine which morphology the barrier will adopt. In areas of bedrock depressions, a barrier will have a shoreface backed by a lagoon and will be able to maintain an inlet and accompanying deltas. In areas of high bedrock topography, the barrier lacks a shoreface and the backbarrier lacks inlets due to the limited basin size (Cooper et al., 2018). Different shoreface morphologies will modify waves and currents, subsequently affecting patterns of erosion, transport, and deposition along the shoreline (Cooper et al., 2018).

The Point Pelee foreland originally formed as a moraine deposited by glaciers. Lake Huron started to flood what is now Lake Erie, and as water levels started to rise, the beach of the moraine continued to move inward, forming the shape of Point Pelee (Trenhaile and Dumala, 1977) (Figure 8). The west side of the moraine had a higher elevation and a deeper subsurface than the east,

where the basement topography was a gentle slope. This original shape helped influence the foreland as it is today, which consists of a low-lying marsh and barrier spit on the east side, and dune and beach system on the west (Figure 7).

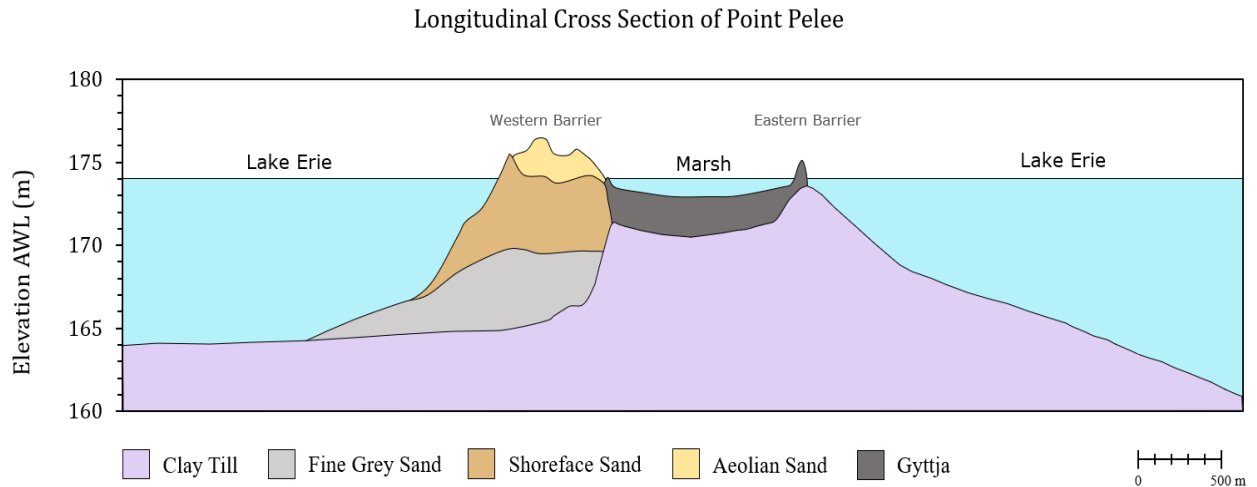


Figure 7: Longitudinal cross section of Point Pelee, adapted from Coakley et al. (1998).

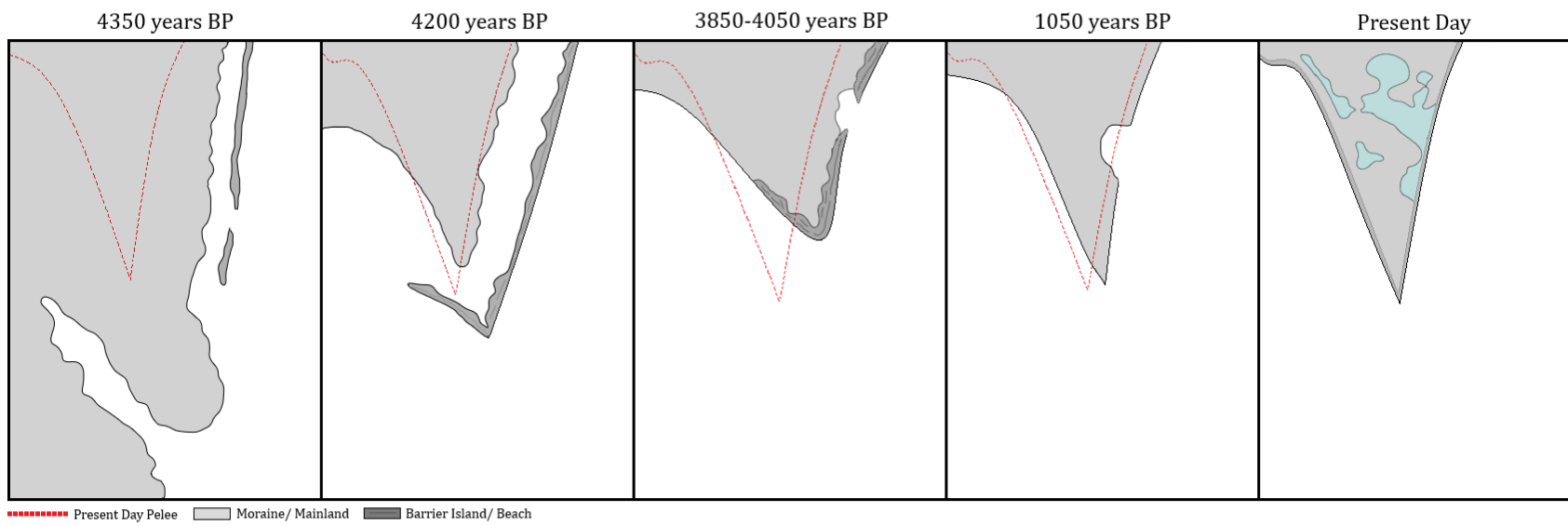


Figure 8: The evolution of the Point Pelee Foreland, from 4350 BP to present day. Adapted from Trenhaile and Dumala (1977).

2.3.3 Sediment Supply

Barrier response to changing conditions is also partly determined by sediment supply. The shelf and shoreface are the most common sources of barrier sand, however high-relief coastlines are dominated by fluvial sediment sources, and paraglacial barriers are dominated by cliff erosion (Cooper et al., 2018). The construction of coastal structures, such as groins and jetties, can disrupt longshore drift, cutting off sediment supply, and resulting in barriers or sections of barriers to retreat on the downdrift side. Vaidya et al. (2015) concluded that the longer the groin, the more sand is trapped, and the more erosion that occurs on the downdrift side. Also, the farther apart groins are in a groin field, the more the shoreline in between is exposed to wave attack. Coastal structures can also disrupt normal processes of wind, wave, and current movement, further impacting sedimentation and erosion patterns in the coastal cell (Airolidi et al., 2005). Nature-based solutions are recommended by environmental specialists as a method of mitigating the risks of climate change without causing environmental harm, as these types of structures rely on their natural ability to stabilize and protect shorelines, attenuate waves, and reduce flood surge (Mamo et al., 2022).

Sediment supply strongly influences barrier volume, in turn controlling barrier inertia, which determines how rapidly a barrier can be reorganized in response to external forces and is measured as a function of sediment volume. Barrier inertia is also affected by barrier elevation, and whether a barrier is low enough to allow for overwash and roll landwards, whereas high and wide barriers do not migrate quickly, although sediment can still pass through aeolian processes (Cooper et al., 2018).

2.4 Barrier Breaching

Breaches can be initiated naturally, due to storms or high water levels, or artificially. Breaches are artificially opened by digging a narrow channel through a barrier, allowing it to deepen, widen and create steep slopes by the rushing water. Their stability relies on consistent strong flows of water or wind. Justifications for artificially induced breaches include reduction in water level to prevent the flooding of nearby properties; altering of salinity levels in a lagoon or bay (situational); promotion of water exchange to improve water quality; and the facilitation of migration of marine organisms (Kraus et al., 2002). Artificial breaches often close naturally, but if wave action is strong, and longshore sediment is weak the breach can continue to widen and become an inlet (Kraus, 2003). For instance, artificial breaching is an annual occurrence at Mecox Bay, Long Island, New York, for almost a century (Figure 9). The annual breach is made to prevent neighboring properties from flooding during water level rises and are left to naturally close by sediment transport (Smith & Zarillo, 1988). In certain cases, if artificial breaches do not close naturally, a new inlet can form and take dominance over the system previously in its place, creating environmental consequences from water level and circulation changes. A new inlet can also give rise to navigation discrepancies (Kraus, 2003).



Figure 9: Annual breaching at Mecox Bay, Long Island, New York, to prevent property flooding.

Barrier breaching occurs in both marine and lacustrine environments, to keep descriptions consistent, lakes and seas will hereafter be generalized as “open water”, and the backbarrier will be referred to as a “lagoon”. Natural breaching can be initiated in three ways; inundation from the open water combined with wave action, elevated water level in the lagoon, and narrowing of a barrier island by sediment reduction. From the seaward side, Pierce (1970) states that natural breaching depends on: 1) elevation of the barrier, 2) width of the barrier, 3) elevation of the surge, 4) duration of the surge, 5) wave height, and 6) wave period. Energy present in the waves is

dissipated along the barrier and general erosion occurs. To cut through the barrier, this wave energy needs to be concentrated along the barrier. Frontal waves often are directed at the widest points of the barrier – the most improbable place for a breach to occur. While these waves are not strong enough to be effective, storm waves are. Storm waves have potential energy by reason of height and remaining kinetic energy that allows for it to be above still-water level in the lagoon. If the flow can be channeled and if frictional losses are minimal, the available energy may cut a channel (Pierce, 1970). The circulation and the rate of advance can lead to a reversal of wind direction, representing an additional cause of natural breaching. If the forward movement of the storm is rapid and the direction reversal is abrupt, then the side of the barrier facing the open water will have a decrease in water levels. The mass of water that was previously banked against the barrier becomes unsupported and is pushed towards the barrier by an offshore wind, resulting in an abnormally high storm surge that raises the water level on the back barrier (Pierce, 1970). The steepened slope on the foreshore of the barrier is increased by the low water levels, which will increase the velocity of the water and make it effective in eroding a channel in the barrier. A relatively narrow barrier can become breached through liquefaction of sediment by water seepage driven by differences in water elevation (Kraus, Militello & Todoroff, 2002). This allows for large volumes of material to be transported offshore and redistributed by open water waves and currents (Pierce, 1970). Natural breaching threatens marine species through loss of habitat, exposure of calm habitat to harsh wave activity, and unwanted change in water level (Kraus, 2003).

The tendency for barriers to breach from the seaward side can be explained by the “breach susceptibility index” (BSI), defined as:

$$BSI = S_{10}/R \quad (1)$$

where S_{10} is the surge level, as defined by water level, for the 10-year storm, and R is the diurnal tidal range (Kraus, Militello & Todoroff, 2002). Small tidal ranges represent sand deficient coasts of low barrier beaches and spits, in an area where wind cannot steadily build dunes – these will be most susceptible to inundation and breaching during storms. Large BSI can be seen on the Louisiana and Texas coasts, specifically at Padre Island, Texas, the longest known continuous barrier island in the world. Breaching and overwash is common here, with 45 temporary breaches recorded after a hurricane in 1933 (Price, 1947). In contrast, a small BSI occurs in the northwest Pacific due to the large tidal range that allows the creation of high and wide beach berms, and a relatively weak storm surge. Areas with a BSI greater than a critical value around unity are more prone to breach from the seaward side (Kraus et al., 2002).

Kraus (2003) idealizes a barrier breach as shown in Figure 10. Solutions can be obtained by the following simplifying assumptions:

- a) Sediment volume is conserved,
- b) The initial condition of the barrier is known (initial dimensions),
- c) Sediment transport can occur at the bottom of the breach and at its sides,
- d) The breach will approach equilibrium if external forces do not intervene,
- e) Longshore sediment transport is weak or can be neglected.

Assumption (e) limits the equation to incipient breaching. Conservation of mass yields the following equations: (2) for breach width,

$$Lz\Delta x = \hat{Q}s\Delta t \quad (2)$$

and (3) for breach depth,

$$Lx\Delta z = \hat{Q}_B \Delta t \quad (3)$$

where L is length of the breach through the coastal barrier, z and x are depth and width of the breach, respectively, t is time, \hat{Q}_S and \hat{Q}_B are net transport rates along the sides (assumed to be equal) and bottom of the breach, respectively. Equation 1 explains that the length of the breach, multiplied by the depth and change in width of the breach is equal to the net transport rate along the sides of the breach multiplied the change in time. Equation 2 suggests that the length of the breach, multiplied by width and change in depth is equal to the net transport rate at the bottom of the breach multiplied by the change in time:

$$\hat{Q}_S = Q_S \left(1 - \frac{x}{x_e}\right), \hat{Q}_B = Q_B \left(1 - \frac{z}{z_e}\right) \quad (4)$$

where Q_S and Q_B are constant maximum transport rates that are not necessarily equal, and x_e and z_e are values of the breach width and depth, respectively, if the breach achieved equilibrium. The parameters of the transport rates in Eq. (4) are time dependent, with the net transport rates going to zero as equilibrium is approached (Kraus, 2003). Net zero transport rates signify that the breach width, depth, and volume are at their near-maximum and become stable.

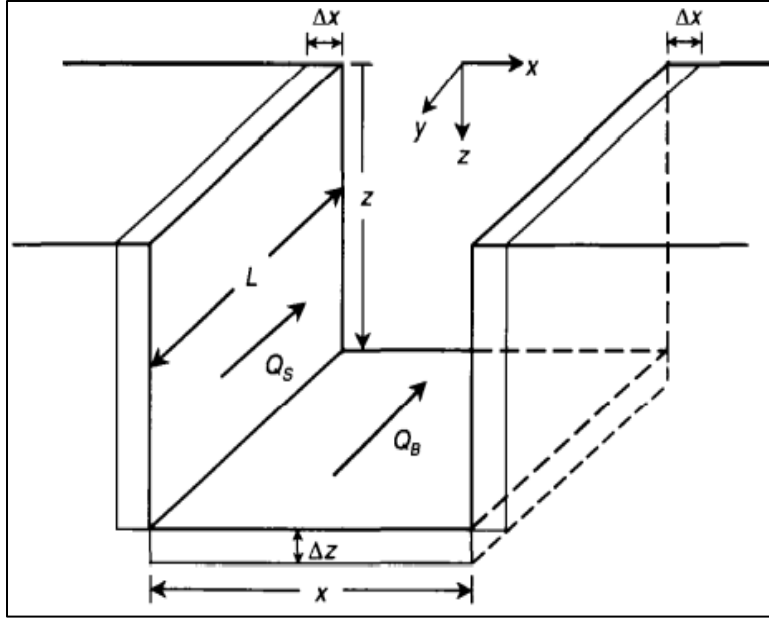


Figure 10: Definition sketch for barrier breaching model proposed by Kraus (2003).

These relationships suggest that the processes associated with the initiation and closure of breaches are determined by the maximum sediment transport rates at the bed and sides of the breach at initiation, and by the equilibrium values of the breach width and depth. The initial dimensions of a breached channel determine the rate at which the growth in volume goes towards equilibrium. Breach growth follows an exponential behaviour governed by a characteristic time scale:

$$\tau = \mathcal{V}e/Q \quad (5)$$

where $\mathcal{V}e$ is the volume of the breach at equilibrium, and Q is the maximum net sediment transport rate through the breach. A breach with larger initial depth will grow towards equilibrium faster and begins to curve at around 30 days. For smaller initial depth, volume grows faster after the initial 30 days due to the larger value of transport rate at the bottom than at the sides. In other words, the model suggests that breach width grows faster for smaller initial depth (Kraus, 2003).

East Beach had an initial breach width 23 m, and increased by 37 m in three months time, while Hillman Beach initially breached at 15 m, and after one year only increased by 15 m.

2.5 Elevated Water Levels

Great Lakes water level fluctuations can be categorized into three timescales: interannual variability, seasonal cycles, episodic events. Interannual variability varies upwards of 2 m and results from long term changes in precipitation and air temperatures, this scale is responsible for record high and low mean lake levels on a monthly basis. The seasonal cycles range from fluctuations of 20 to 40 cm, and are driven by water supply components, precipitation, lake evaporation, changes in channel ice (lags and jams), and lake regulation (source). Episodic lake level changes are a result of storm surges on the lake and ice jams in the connecting channels, and vary from 50 cm to 3 m (Quinn, 2002). In many cases, barrier breaching is associated with extreme storms including meteotsunamis and high-water level storms.

The absence of tides in the Great Lakes attributes to morphological differences between the barrier of the Point Pelee Foreland, and inlets that are facing the ocean. While oceanic barriers are controlled by tides, lacustrine barriers are controlled by wind set-up, wave and current processes, and storm surge. Lake levels vary through meteotsunamis, meteorologically generated water waves of heights above 0.3 metres with periods of less than 2 hours. Meteotsunamis have similar temporal and spatial characteristics to seismic tsunamis, but occur in regions with low seismic activities, such as the Laurentian Great Lakes (Bechle et al., 2016). These waves are mainly caused by atmospheric pressure and wind perturbations associated with frontal passages (Tanaka, 2009), cyclones (Mercer et al., 2002) and atmospheric gravity waves (Monserrat et al., 1991). Perturbations in wind stress and air pressure act on the water's surface to initiate a meteotsunami wave. If the atmospheric perturbation speed matches the speed of the wave, the

height of the meteotsunami wave significantly grows. Growth is also influenced by nearshore wave transformations such as shoaling, refraction, reflection, and superposition (Linares et al., 2019). Meteotsunamis generally come about from the late-spring to mid-summer, coinciding with the recreation season and putting lake users at risk (Bechle et al., 2016).

Abrupt changes due to high water levels during these storm events prevents the ability for barrier elevation to slowly adapt to water level rise, making coastal habitats more vulnerable to erosion (Theuerkauf and Braun, 2021). Climate change in the Great Lakes is projected to increase the variability of water level fluctuations, where water levels will rapidly shift between lows and highs. These rapid changes are suggested by Theuerkauf and Braun (2021) to be the main driver of large habitat loss via erosion and overwash burial. High water levels alone are not enough to drive this change, it must be a change of high magnitude or be associated with an increase in wave energy. Mid-latitude cyclones are low-pressure weather systems where warm and cold air masses meet in the middle latitudes of the North and South Hemispheres (Porterfield, 2021). These storms are the driving force behind the strong winds that create high wave storm events on the Great Lakes. Meadows et al. (1996) emphasize that these climate change driven high lake levels lead to increased precipitation or reduced evaporation and transpiration. After observing storm damage along the Great Lakes coasts, they also conclude that increases in mean lake levels are correlated with increased total wave energies, the primary cause of severe shoreline damage.

2.6 Lake Ice Coverage

Lofgren et al. (2002) suggests that the temperature increase resulting from climate change will cause a significant reduction in ice cover, predicting that Lake Erie will have 96% of its winters ice-free by 2090. Winter ice can have two potential effects: protection from erosive waves, or intensification of future erosion by the alteration of near-bottom topography. In periods of

consistently below freezing temperatures, an ice foot forms along the beach, blocking waves, freezing the beach and preventing sediment loss through wave action (Figure 11). Sediment entrained in the ice ends up being transported offshore as the ice melts, causing a local net sediment loss (BaMasoud & Byrne, 2012). In a case study along the Point Pelee shore, BaMasoud and Byrne (2011) conclude that ice coverage protected the shoreline from erosion, resulting in sediment accumulation, and substantial erosion took place where ice was absent. The Point Pelee Foreland is in the western basin of Lake Erie, and due to its shallower bathymetry (relative to the central basin) and shorter fetch length (subsequently created smaller waves that cause less erosion), it is protected by ice for a longer period, however, this is currently threatened by climate change.



Figure 11: Ice cover on Lake Erie, around Point Pelee National Park, taken January 25th, 2022. Ice cover protects shorelines over the winter from erosion by limiting fetch distance across the lake.

2.6.1 Under-Ice Currents

While hydrodynamic processes in ice-covered lakes are only sparsely studied, Malm et al. (1998) describes four different types of under-ice currents. River through-flow induced currents are present in large rivers with narrow lakes, and their processes are analyzed similar to that of channel flow. These are distributed over the entire width of the lake. Oscillating currents are generated through aeolian processes on the ice cover, causing it to tilt and oscillate. These currents have periods similar to the estimated seiche period (3-4 mm/s). A bottom current is generated by the heat transfer of bottom sediments, and this now warmed warm and dense water moves along the bottom towards deeper parts of the lake. Indirect dye measurements were taken and found the velocity of bottom currents to be on the order of 0.11 mm/s or less. Lastly, convective currents can be generated by the penetration of solar radiation into the water when the ice is snow-free or when there is minimal snow cover. This short-wave radiation leads to hydrodynamic instability and a homogenous temperature layer. Convective currents were found to have a velocity of between 0.6 mm/s to approximately 2mm/s (Malm et al., 1998).

Although breaches are covered in ice over the winter, further research is required to understand the potential effect of these currents on shoreline erosion during ice-cover seasons. Studies show that these currents are of small magnitude and on the order of millimetres per second, but none have looked at whether they directly affecting the widening or opening of breaches.

2.6.2 Ice Scouring

As lakes thaw and ice-cover begins to melt, fragments of ice can scour beach sediment and transport it offshore, making the nearshore slope more susceptible to erosion and exposed to higher wave activity. When the barrier bar is more shallow and the slope is smaller, these sediments can

be slowly redistributed back onshore during calm conditions and low open water levels. In contrast, deep bar with steep slopes will experience significant erosion at the beginning of the ice-free season as sediments will continue to be transported offshore rather than being redeposited onshore (Smith and Houser, In-Review). This further exposes the shoreline to high wave energy and erosion, potentially leading to breaching as ice scouring alters the elevation and width of the barrier.

2.7 Barrier Breach Examples

As barrier breaching is a relatively less researched process, it is difficult to pinpoint when a breach will open and how it will close. Past studies have given hypotheses or were able to closely pinpoint what causes breach closure. Safak et al. (2016) monitored a breach at Pea Island, on the outer banks of North Carolina, facing the Atlantic Ocean. A breach occurred here during Hurricane Irene after wind and wave setup at the ocean side brought the water level to -0.1 m AWL. This created a 2.2 m difference between the bay and the ocean water levels, creating a breach (Figure 12). Between the opening from Hurricane Irene and widening of the breach during Hurricane Sandy, the gross alongshore transport rate was about 400 km³/y. Post-Sandy, the gross alongshore transport rate increased by 50% and this considered the reason for the breach closure (Safak, Warner & List, 2016). At Carmel River, along the California coast, barrier breaching occurs commonly during the rainy season as the water levels on the lagoon side slowly increase until they overtop the beach and create a breach. Since there is always an offshore pressure gradient between water levels in the lagoon and the tide, water is inclined to flow from the lagoon and out to the ocean, with discharge rates above 100 m³/s and often exceeding 1000 m³/s. If tides and breaking waves from the ocean side stay sufficiently weak the breach will remain open. Water level analysis

determined the closure of the breach was attributed to strong ocean forcing which balanced the offshore pressure gradient (Orescanin & Scooler, 2018).

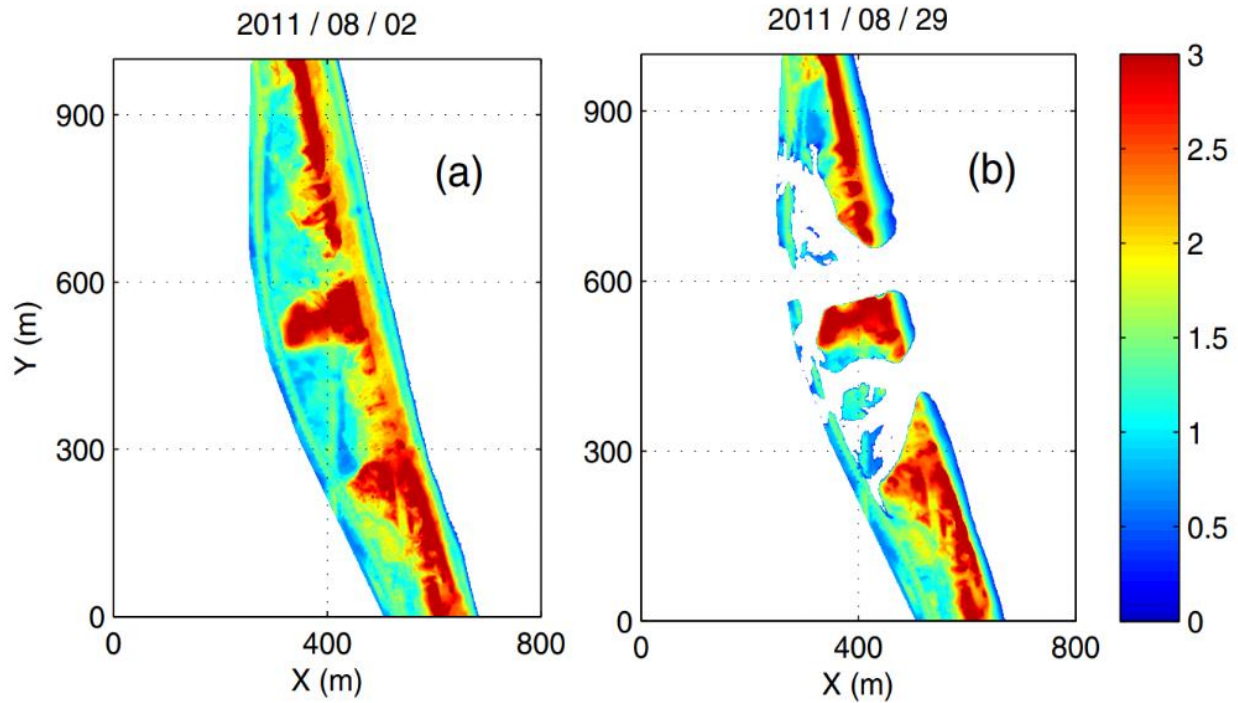


Figure 12: Topography near Pea Island, North Carolina, (A) before and (B) after Hurricane Irene.

At Bayocean Peninsula, west of Portland, Oregon, a jetty was constructed at the northern end to provide a reliable navigation channel, and erosion continued at a rate of 6.1 m/year until a storm breached the barrier at its narrowest and lowest point. This breach was artificially closed by coastal engineers through sand and rock fill, with rocks being the focus. The rock fill was built 6.1 m tall and 4.6 m wide, it stretched across the entire channel at 243.8 m long (Wamsley & Kraus, 2003). Artificial closure was also a success at the Buxton Inlet, North Carolina, where the “Ash Wednesday Storm” created a breach that destroyed a coastal road that connected the residents of Avon from Buxton where children attended school. Two attempts were made to pump sand with a hydraulic pipeline dredge from both sides of the breach, however, the first attempt’s pumping

capacity was not sufficient to overcome scour as the breach goes through the process of closing. A second pipeline dredge was employed, and local interests dumped broken automobiles, culverts and other nonengineered materials to try and stop help the flow. Once the second dredge finally reached the site a few months later, the breach was able to help close the breach in 3 days (Wamsley & Kraus, 2003). Previous case studies show how quickly breaches can expand, especially if there is limited sediment supply and strong offshore currents, and subsequently become million-dollar repair projects.

2.8 Variations in Fish Species Composition due to Breach Events

Species in isolated areas, such as backbarrier lagoons, will become locally extinct over time, due to stochastic events, habitat change, predation, or resource scarcity, resulting in a decline in species richness. Young and Potter (2003) compared changes in the fish species composition before and after an artificial breach was created in a large estuary, observing that the construction of the channel led to a decline in the inter-annual variations in the species richness and similar fish species composition over time.

Breach events can directly impact the physical and chemical composition of marsh ponds through the addition of water from the lake, including sediment accumulation, concentration of pollutants, higher temperatures, reduced water depth, and higher dissolved oxygen demands (Surette, 2006). These new conditions may favour some species over others, and cause the indirect impact of immigration and emigration, inducing considerable variation in species composition that will in turn introduce predators and competitors, introducing or extirpating native species. This causes long-term changes in the composition of fish assemblages (Surette, 2006). Surette (2006) suggests that infrequent breaching at Point Pelee may naturally restore its ecological integrity, as fish assemblages will become more dissimilar over time.

3. Purpose and Objectives

3.1 Chapter One: Historical Changes on the Point Pelee Foreland

The objective of this study is to examine historical aerial imagery between 1931 – 2020 and lake level fluctuations on a decadal to centennial scale to establish the controls on barrier transgression, overwash, and breaching occurring at East Beach in Point Pelee National Park and Hillman Beach in Hillman Marsh Conservation Area. This study will also examine the initiation, expansion, and closure of breaches located on the eastern shore of the Point Pelee Foreland in response to the 2013-2020 period of lake level rise. A conceptual model will be developed on the cycle of barrier beach breaching and evaluated on the ability to predict breaching at mentioned study sites.

3.2 Chapter Two: Breaching Patterns at Hillman Beach and East Beach

This objective of this chapter is to further analyze collected data and determine breaching patterns at both East Beach and Hillman Beach. This chapter also compares the different patterns at both sites and suggests the controls that result in the different behaviours. A four-step conceptual model is proposed on natural breaching in lacustrine environments and contrasted to a conceptual model for a modified shoreline.

4. Study Site

This study focuses on two of Point Pelee's eastern barriers located at Hillman Beach (HB), part of the Hillman Marsh Conservation Area (Figure 14B), and the central section of East Beach (EB), located within Point Pelee National Park (Figure 14C). Point Pelee is a ~50 km² foreland that separates the Western and Central Basins of Lake Erie, projecting approximately 15 km southward from the shoreline of Essex County, Ontario (Figure 14A). Point Pelee National Park is located on the foreland extending up to 9.0 km from north to south and up to 4.2 km from east to west (BaMasoud & Byrne, 2011). Point Pelee has a unique Carolinian Forest, beach, dune, and marsh ecosystem that provides critical habitat for rare and endangered species (Drezner, 2021). The marsh is enclosed by a series of ridges to the west and a single ridge to the east. Point Pelee was formed over the Pelee-Lorraine moraine by the enclosure of the marsh by the eastern and western barriers ~3500 years BP, following a period of rapid lake level rise (Trenhaile and Dumala, 1977).

Sediment is supplied towards the foreland tip through erosion of glacial bluffs (Figure 15A) and alongshore drift, from the Colchester to Southeast Shoal littoral cell in the west, and the Port Alma to Southeast Shoal littoral cell in the east (Trenhaile et al., 1998; Figure 13). The western side of the foreland is exposed to a relatively low wave energy environment due to the limited fetch in the western basin, whereas the eastern side of the foreland is exposed to a higher wave energy environment as a result of a fetch distance of up to 300 km. In response, the western barrier consists of a prograding shoreline and a series of dune ridge and swales, while the eastern barrier is regressing and consists of a single beach ridge (Trenhaile and Dumala, 1977). Between 1954 and 2005, the western barrier prograded by 0.4–0.2 m y⁻¹ while remaining relatively stable at the southern extent, and the eastern barrier transgressed by -3.14 m y⁻¹ in the north and -1.03 m y⁻¹ in

the south (BaMasoud and Byrne, 2011). Given the relative stability of the western shoreline, this study will focus on the eastern barrier system and specifically the breaches at HB (Figure 14B) and EB (Figure 14C).

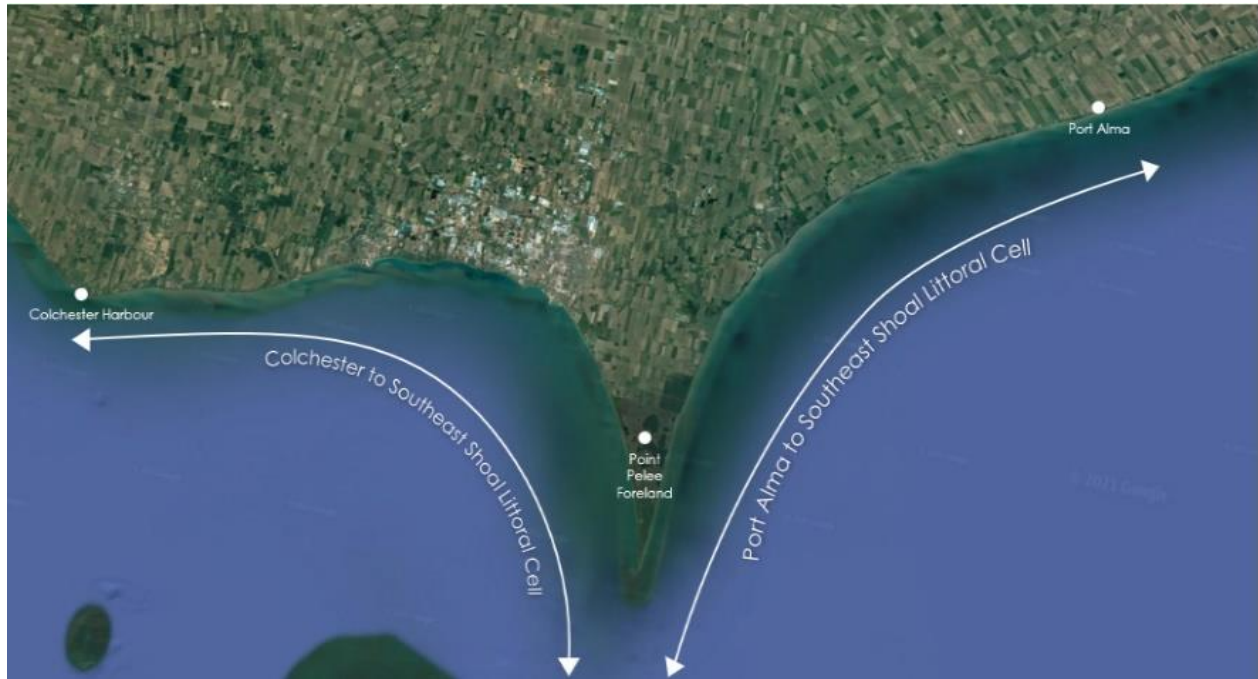


Figure 13: Sediment is supplied through alongshore drift, from the Colchester to southeast Shoal littoral cell in the west, and the Port Alma to Southeast Shoal littoral cell in the east.



Figure 14: This study is conducted on (A) the Point Pelee Foreland, specifically at (B) Hillman Beach (HB) and (C) East Beach (EB).



Figure 15: (A) Glacial bluffs located between Port Alma and Wheatley Harbor are the primary source of sediment in the Port Alma to Southeast Shoal littoral cell that supplies the eastern barrier of Point Pelee. (B) Wheatley Harbor and Jetty has trapped or removed $\sim 500,000 \text{ m}^3$ of sediment from the littoral cell causing an increased sediment deficit of the downdrift shorelines (Baird, 2007). (C) Hillman Beach was breached during the current high lake level period and has expanded rapidly and eroded most of the central and southern barrier. (D) Shoreline retreat at Hillman Beach has resulted in vegetation and tree loss. (E) and (F) show the aerial and ground view of the breach at East Beach.

Over the last century, the yearly average water level (AWL) for Lake Erie was 174.16 m; however, ~0.4–1 m fluctuations regularly occurred between decadal water level highs and lows throughout this period (Figure 17, Great Lakes Environmental Research Laboratory). Additionally, wave data was taken from NOAA's National Data Buoy Center for Station 45005, located ~25 km SSE of Point Pelee. Oblique to onshore significant wave heights (generated from the NNE – SSE) indicate an increase in erosive potential between the late autumn and early spring seasons, although lake ice coverage during winter may mitigate coastal erosion at Point Pelee (BaMasoud and Byrne, 2011, 2012). While the eastern barrier is sheltered from wind waves from the west, the highest magnitude average significant wave heights of ~0.65 m were recorded from the NE. Sedimentation rates and barrier transgression within the region have been further affected by human development including the construction of Wheatly Harbor and Jetty (Figure 15B) that has trapped or removed ~500,000 m³ of sediment from the Port Alma to Southeast Shoal littoral cell (Figure 13), and stabilized rock armored coastlines on the southern extent of Hillman Beach (Figure 16) (Baird, 2007; Trenhaile et al., 1998).



Figure 16: Rock revetment put in place by the City of Leamington in early November 2020.

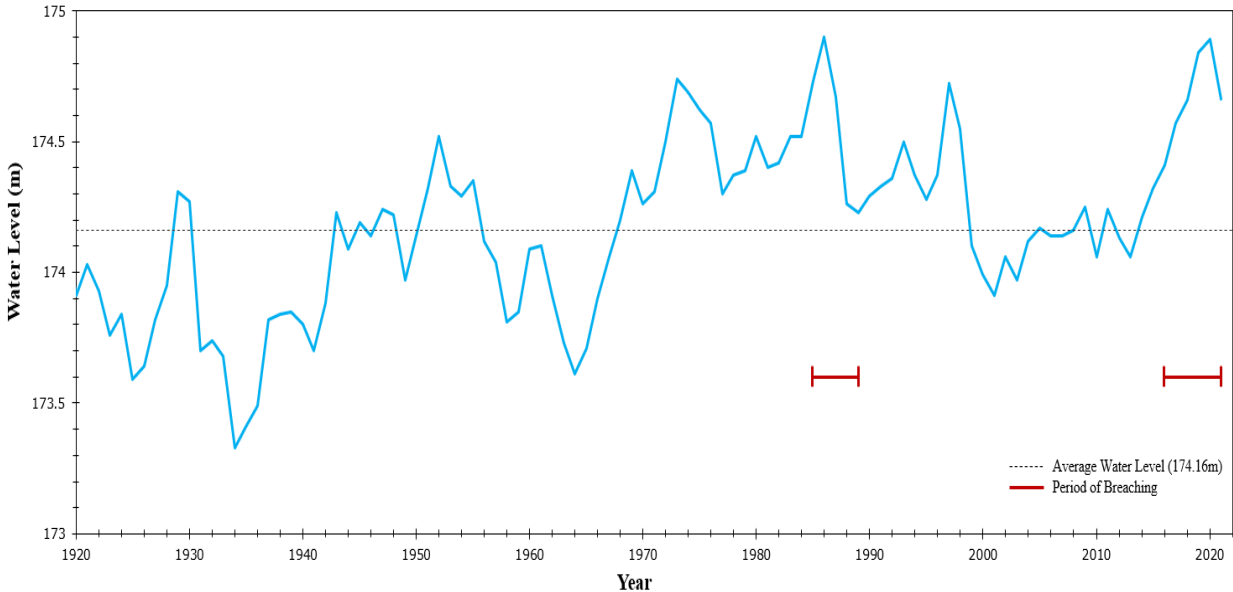


Figure 17: Lake Erie annual average water levels from 1920 to 2021. Data gathered from Great Lakes Environmental Research Laboratory.

5. Methodology

Previously published reports and aerial photographs were gathered to assess the history of shoreline retreat. Historical aerial photographs of Point Pelee National Park (PPNP) and Hillman Marsh Conservation Area (HMCA) were gathered from Parks Canada (PC) and Earth Observation Data Management System (EODMS). All photographs were georeferenced to the projected coordinate system NAD 1983 UTM Zone 17N.

To supplement this data, Unmanned Aerial Vehicle (UAV) surveys are taken every two months with a DJI Mavic 2 Pro, using the Pix4DCapture application. These flights were conducted in a series of overlapping grids at a height of 55 metres and maintained a ground sampling distance of approximately 1 cm per pixel. White bucket lids (30 cm diameter, Figure 18) were used as Ground Control Points (GCPs), distributed randomly, and were assigned specific UTM coordinates using a Real Time Kinematic (RTK) capable GPS receiver. These were georeferenced to increase the accuracy of the orthomosaics produced in post-processing, and GCPs with high error were removed. Flights were processed using the Structure from Motion (SfM) Pix4DMapper software to generate a point cloud, orthomosaic, and digital surface model (DSM). Noise filtering was used to correct the altitude of the points to avoid inaccurate points while generating the DSM, as well as sharp surface smoothing to correct areas with small erroneous bumps, while still preserving the orientation of the surface and keep sharp features such as rock walls and wave breaks. The DSM and orthomosaic were generated with a resolution of 1 cm/pixel, using the triangulation algorithm based on Delaunay triangulation, as this is more suitable for flat areas and works up to ten times faster.



Figure 18: Ground Control Points (GCPs) in use during a survey at East Beach in August 2020. GCPs are assigned specific UTM coordinates using a Real Time Kinematic (RTK) capable GPS receiver, are georeferenced to increase the accuracy of the survey.

The shoreline positions were digitized for East Beach were for the years 1931 – 2021, and Hillman Beach for 1973 – 2021. Table 2 indicates each dataset source and resolution. Sources include Parks Canada (PC), Google Earth Pro (GEP), Essex Geocortex (EG), and Earth Observation Data Management System (EODMS).

Table 2: Yearly aerial imagery source and resolution.

Year	EB Imagery - Resolution (m)	Source	HB Imagery - Resolution (m)	Source
1931	0.25	PC	-	-
1959	0.25	PC	-	-
1973	0.25	PC	1	EODMS
1974	-	-	1	EODMS
1975	-	-	1	EODMS
1976	-	-	1	EODMS
1977	0.15	PC	-	-
1980	-	-	1	EODMS
1985	1	PC	-	-
1988	-	-	1	EODMS
1989	-	-	1	EODMS
1990	1	PC	-	-
2000	0.1	PC	-	-
2004	0.1	PC	-	-
2006	0.3	PC	-	-
2009	0.87	GEP	0.95	GEP
2010	0.2	PC	-	-
2012	-	-	0.95	GEP
2013	0.3	PC	-	-
2015	0.2	PC	-	-
2016	0.1	PC	0.96	GEP
2017	0.1	PC	0.96	GEP
2018	0.1	PC	-	-
2019	0.1	PC	-	-
2020	-	-	0.6	EG
2021	0.6	EG	0.6	EG

Using ArcMap, a new feature class was created for every available year and the shoreline was manually digitized as a line feature by identifying the “wet-dry boundary” (Boak and Turner, 2005) at a scale of 1:400 to capture small scale variability in coastline orientation. Once every

shoreline was digitized, historical shoreline retreat for these two sites could be visualized and measured. A series of geo-located transects were generated 1 m apart, alongshore at an angle perpendicular to the coast, 1475 transects were generated at HB and 2417 transects at EB. Shoreline retreat was quantified by calculating the linear regression rate (LRR) and the end-point rate (EPR) of shoreline change (Dolan et al., 1991). The EPR method calculates the distance of total shoreline movement between two images, divided by the time elapsed between those measurements, and averaging those rates of change across the time series. While the EPR is a widespread method that is easy to compute, any error in the data can have a strong impact on the results, and temporal variation can be overlooked in using only two shorelines at a time (Dolan et al., 1991). The LRR method calculates the line of best fit to determine the rate of shoreline change across the time series. This method is based on accepted statistical concepts, is easy to employ, and uses all the data to calculate change, rather than just two. However, with this method, clustered shorelines may have more influence on the regression than others, for example, several modern shorelines in a series with only a few old shorelines may lead to skewed results (Dolan et al., 1991).

After collecting the first year of data and quantifying shoreline change, UAV surveys were continued to monitor shoreline change and breaching at EB and HB. Supplementary data was collected through the National Oceanic and Atmospheric Association (NOAA) and analyzed in Microsoft Excel and ArcGIS. This included barrier width, barrier length, vegetation cover, Annual Maximum Ice Cover, marsh area, median fetch distance, nearshore slope, wind direction (based on fetch and on the circular mean), wind speed, and wave height.

6. Historical Changes on the Point Pelee Foreland

6.1 Results

6.1.1 Hillman Beach barrier (1973–2020)

Shoreline changes were monitored along a ~1.5 km section of HB between 1973 and 2020 (Figure 19). From a total of 1475 transects spaced every 1 m alongshore, the average end-point rate (EPR) and linear regression rate (LRR) were -1.35 m/y and -1.06 m/y of shoreline transgression over this period, respectively, with an R^2 value of 0.80. In general, the rate of transgression increased moving northward towards the updrift end of the barrier. Although the time series is not continuous, it does include a range of lake level fluctuations relative to the longer-period average water level (AWL) of Lake Erie. Due to the increased accuracy of LRR over EPR, transgression rates moving forward are calculated through LRR.

In 1973, water levels peaked at +0.58 m (relative to AWL) before slowly falling to +0.45 m in 1975 and to +0.41 m in 1976. During this period of high lake levels, shoreline retreat was well above longer-term averages at -4.92 m/y, small ~20 m breaches can be observed on the southern (1973) and northern (1976) ends of the barrier, and overwash deposits were visible along the back barrier (1975). A record water level peak occurred in 1986 at +0.72 m, however, imagery was not available until 1988 when water levels had already fallen to +0.1 m. A relatively small ~20 m breach is evident in 1988 with the landward transfer of sediment visible in the lagoonal water column and by the considerable accumulation of sediment in the lobate downdrift end of the breach. By 1989, water levels fell to +0.06 m, the breach closed, and shoreline progradation of 9.35 m/y significantly increased the width of the barrier. This is particularly evident in areas adjacent to the former breach which also expanded landward and became the widest section of the

barrier. The landward migration of the breach formed a localized concavity in the shoreline that appears to act as a sediment sink as lake levels dropped. Following another water level peak in 1997 at +0.55 m, a prolonged period of near-AWL and stable water levels occurred between 2001 and 2013. By 2009, shoreline transgression was slightly less than the longer-period average at -0.95 m/y, although a noticeable increase in vegetation cover occurred on the back barrier and in areas of former disturbances (i.e., breaches and overwash) suggesting this was a period of relative inactivity. Water levels rose in 2016 to +0.25 m and in 2017 to +0.42 m. During this period, a small ~30 m breach opened near the same location as the breach in 1973 and shoreline transgression increased to -2.95 m/y. In 2020, lake levels matched the previous 1986 record at +0.72 m, shoreline transgression accelerated to -5.46 m/y, and the breach significantly expanded to the largest on record at ~320 m. Much of the southern end of HB has been entirely eroded, herbaceous and woody vegetation removed, and the marsh exposed to fully developed lake waves.

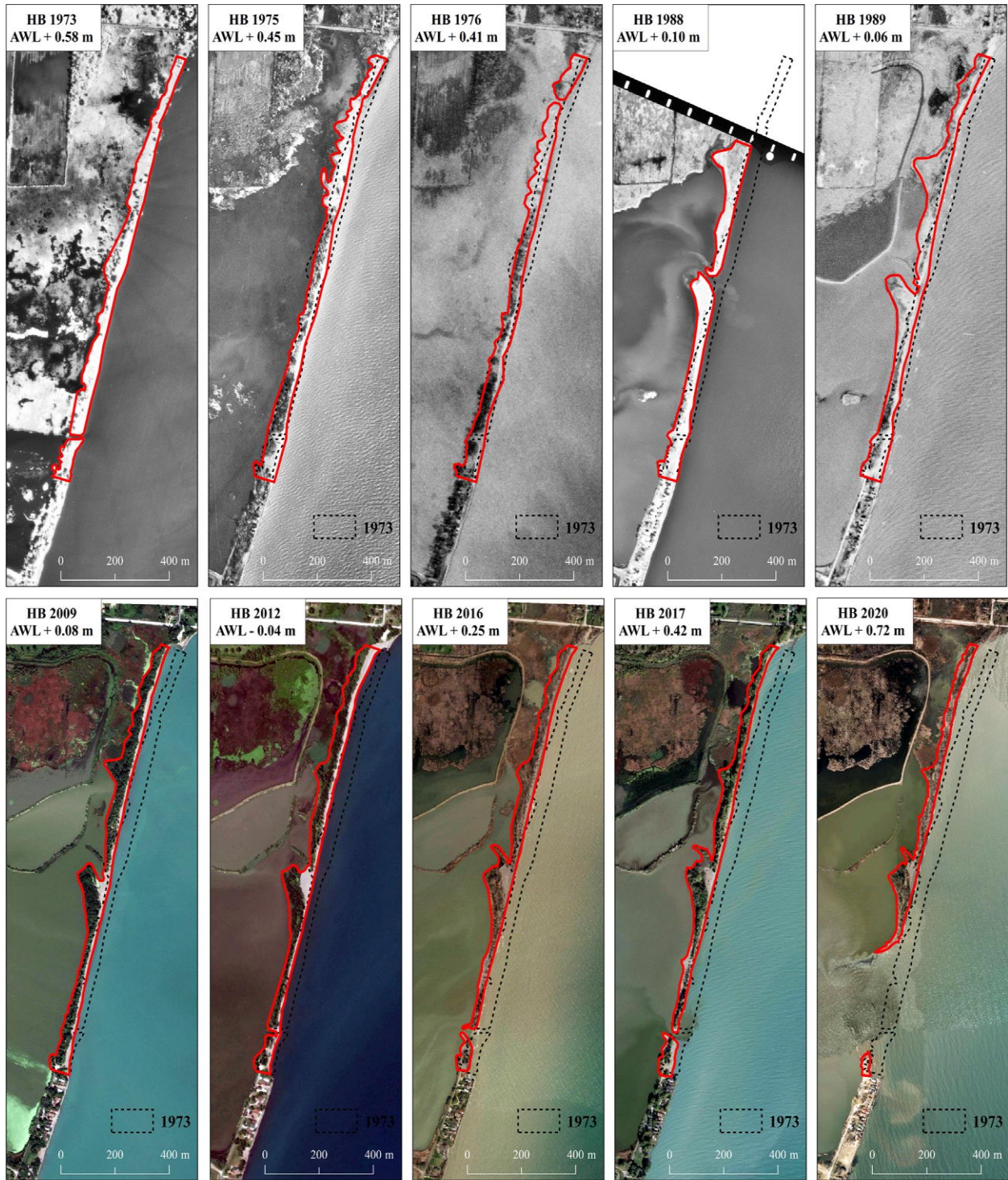


Figure 19: Historical changes at Hillman Beach (HB) between 1973 and 2020. Patterns of barrier transgression, overwash, and breach initiation and closure can be observed in response to lake level fluctuations relative to the longer-period Lake Erie average water level (AWL).

6.1.2 East Beach barrier (1931–2019)

Shoreline changes along a ~2.4 km section of East Beach (EB) Barrier were monitored between 1931 and 2019 (Figure 20). A total of 2417 transects recorded shoreline change throughout this time with an EPR and LRR of -1.76 m/y and -1.22 m/y, respectively, with an R^2 value of 0.78. Similar to HB, an increase in transgression rates were recorded moving north along the updrift shoreline where the narrow beach ridge retreated into the marsh. The mid-section of barrier fronting Lake Pond transgressed at a relatively slower rate, however, the width of this section of EB appears to fluctuate considerably with barrier narrowing, breaching, and widening occurring through time. Given the discontinuity in the sequence of aerial imagery, changes to the barrier will again be interpreted relative to AWL to determine the barrier response to decadal water level cycles.

In the baseline 1931 imagery, lake levels fell from a +0.15 m peak in 1929 and were the lowest level within the observational record at -0.46 m. During this time, EB was at its furthest lakeward extent and maximum width in the middle and southern sections of the barrier. Following a four-decade period of lake levels that were largely at or below AWL and a below average rate of transgression of -0.46 m/y, a +0.57 m peak occurred in 1973 that coincided with a narrowing of the barrier fronting Lake Pond. Lake levels fell to +0.13 m by 1977, although EB experienced further narrowing, accelerated transgression rates of -3.52 m/y, and overwash fans became visible along the backbarrier at the northern end of Lake Pond and adjacent marsh. By 1985 lake levels peaked at +0.56 m, transgression rates increased to -4.55 m/y, a ~40 m breach formed in the mid-section of EB, and landward sediment transport through the breach was visible in Lake Pond. Lake levels fell to +0.12 m by 1990, and the breach closed. Landward of the former breach, a significant amount of sediment accumulation occurred on the backbarrier, likely through storm-induced

overwash deposits, increasing the width of this section of EB following closure. Between 2000 and 2013, a prolonged period of stable and below AWL lake levels occurred, the shoreline convexity lakeward of the former breach filled-in and became the widest section of the barrier, vegetation colonized areas that were previously breached or overwashed, and transgression rates were below longer period averages at -0.75 m/y. In 2016, lake levels rose to +0.24 m and shoreline transgression increased to -2.95 m/y. Lake levels peaked by 2019 at +0.67 m and increased transgression rates of -5.36 m/y were observed. Additionally, a ~77 m breach formed at the northern end of Lake Pond and overwash fans were deposited in the adjacent marsh.

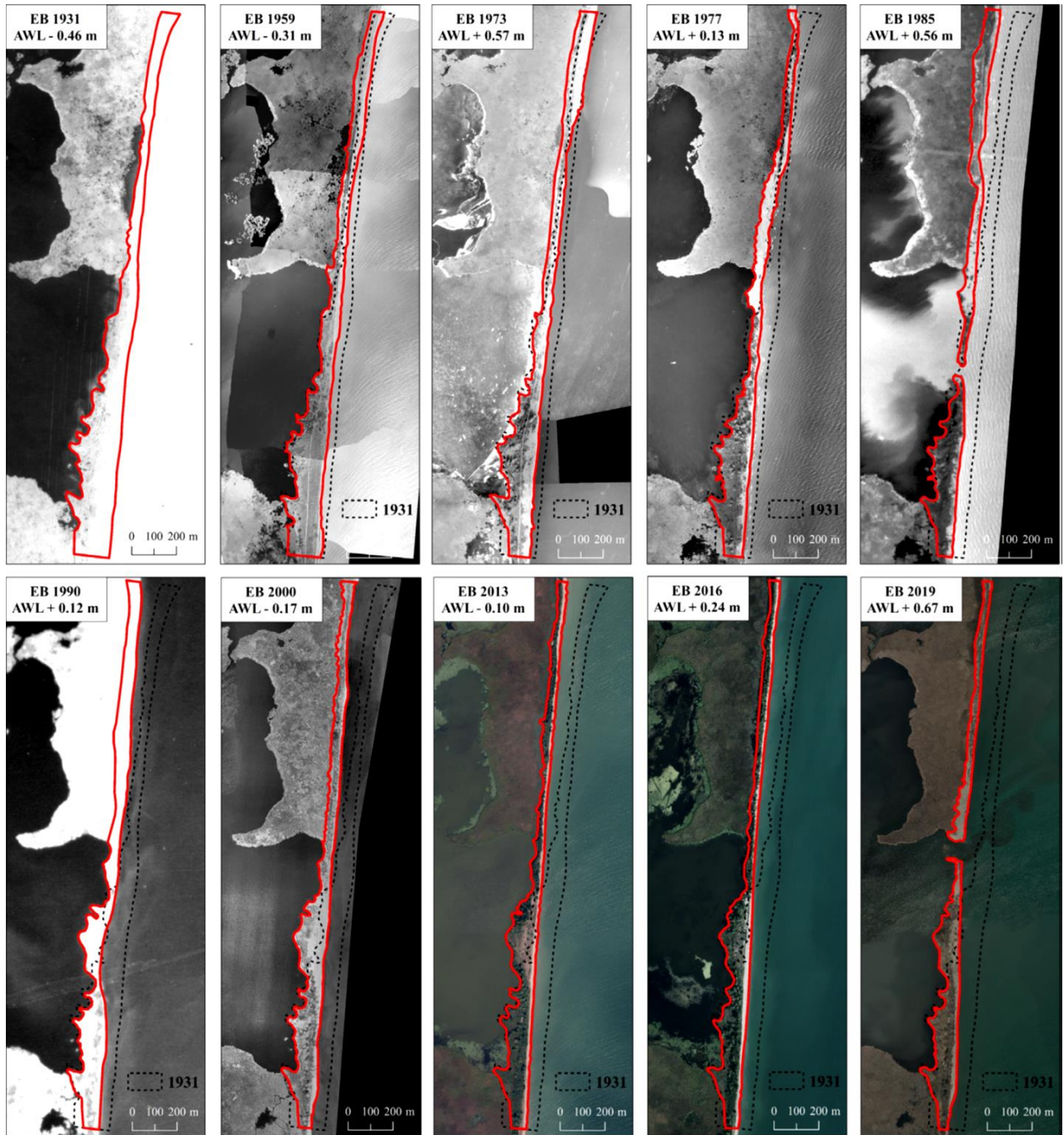


Figure 20: Historical changes at East Beach between 1931 and 2019. Patterns of barrier transgression, overflow, and breach initiation and closure can be observed in response to lake level fluctuations relative to the longer-period Lake Erie average water level (AWL).

6.1.3 Breach initiation, expansion, and closure (2016–2020)

Following over a decade of lake levels that were relatively stable and below AWL, an increase in lake levels began in 2013 from -0.1 m to a record high of +0.72 m in 2020. The breach at East Beach (EB) was first reported in 2017, forming during this period of lake level rise. By 2019, the breach was ~77 m and sediment started to accumulate on the pond side of the breach channel. In August of 2020, a spit formed extending from the northern end of the breach into the center of the former channel (Figure 21 and 22A). The southern end of the breach rotated and moved landward and became separated from the northern spit by a narrow channel, decreasing the width of the breach to ~15 m (Figure 21 and 22B). Further south, the narrow barrier is just above lake level, although a greater volume of sediment is observed just offshore in this downdrift section of the breach (Figure 21 and 22C).

Following the August 2020 survey, the breach was reported closed by the staff at Point Pelee National Park by October 27th. Buoy data indicates that starting on October 25th, northeasterly wind driven waves occurred over a ~24 h period with average and peak significant wave heights of 1.03 m and 1.52 m, respectively. While the exact process for closure is unknown, it is likely that this higher wave energy period contributed to the breach fill-in by accelerating the rate of alongshore drift or mobilizing sediment located further offshore. Storm surge due to wind set-up likely contributed to above average (174.72 m for October 2020) water levels, however, local water gauges at Kingsville and Erieau, operated by Fisheries and Oceans Canada (DFO), are located either in the lee of the foreland for the former or parallel to prevailing winds for the latter. Only a relatively small increase in water levels, relative to the monthly average, were recorded at Kingsville (+0.17 m) and Erieau (+0.06 m) and likely underestimate water levels on the eastern shore of Point Pelee during the storm event. Following the storm event, a sediment ridge up to ~40

m in width was observed welded onto the lakeside of the former breach as of November 2020 (Figure 21).

At Hillman Beach (HB), a ~15 m breach was first observed in 2016 as lake levels rose (Figure 21). By 2017, the breach expanded to 31 m wide, three years later, the breach expanded significantly to a record ~320 m in the fall of 2020. During this period, average significant wave heights were below the long-term average at 0.48 m and no extreme storm events were identified from the buoy data. However, these records do not include wave conditions from January through March as the buoy is retrieved during the winter months. The winter of 2019/2020 had a near record low maximum ice extent of 15% (Figure 3), compared to the longer-term average of 81%. Low winter ice coverage during the higher energy wave season has been observed to accelerate shoreline retreat around Point Pelee (BaMasoud and Byrne, 2012) and may have contributed to the rapid expansion of the breach. The rock armored shoreline protecting homes further south on HB, now extended to protect the remnant spit at the southern end of the breach, has been stable following the 1970s and is ~35 m lakeward of the adjacent shoreline as of 2020. Given the bistability of the system, it is unclear if it can maintain the historical breach and recovery processes or if the barrier will return to its current position at the southern extent once lake levels fall.

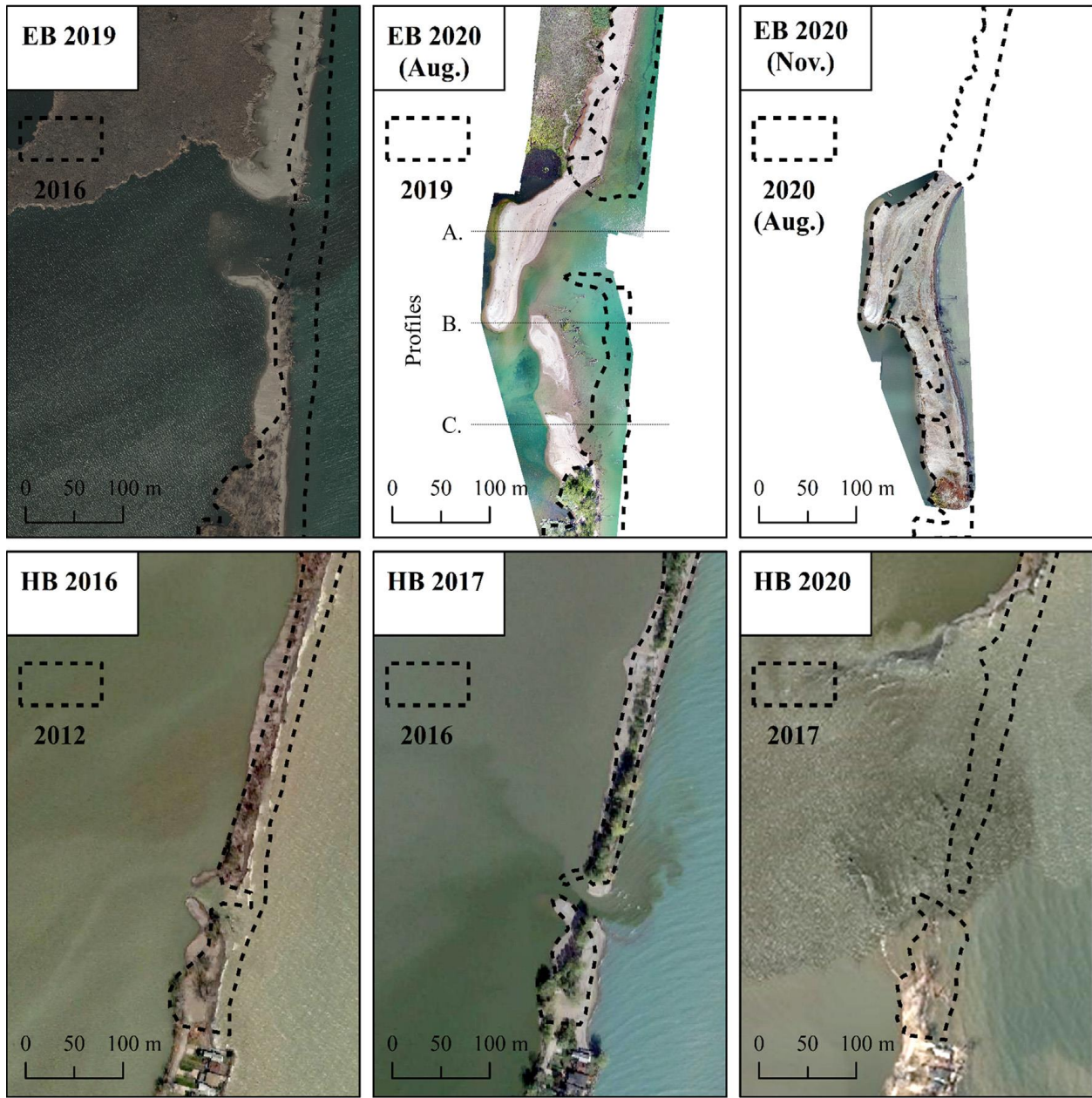


Figure 21: Examples of barrier breach initiation, expansion, and closure occurring at East Beach (top row) and Hillman Beach (bottom row) during a 2013 – 2020 period of lake level rise.

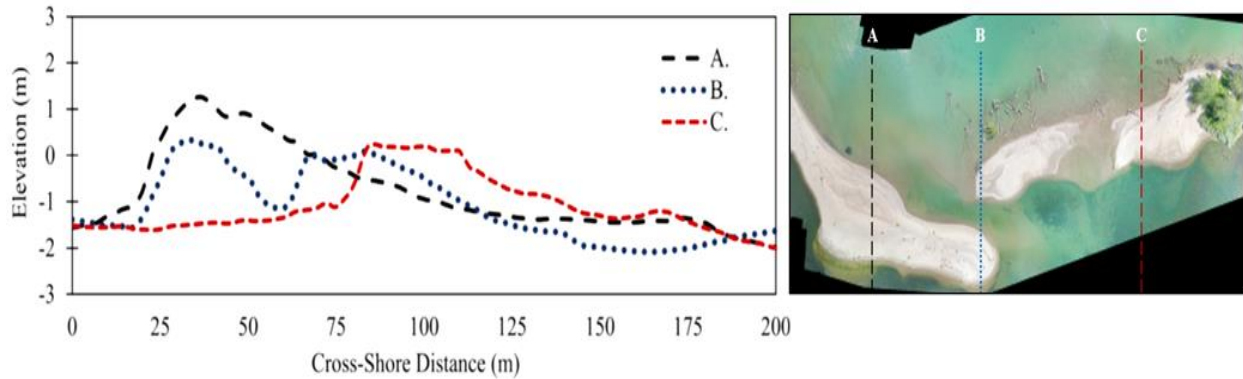


Figure 22: Profiles extending from Lake Pond, across the breached barrier at East Beach, and into the nearshore of Lake Erie. All three cross-sections are from a UAV survey in August 2020. Profile A from the northern end of the barrier, profile B from the centre, and profile C from the southern end of the barrier.

6.2 Discussion

Historical aerial imagery between 1931 and 2020 were used to examine decadal scale changes occurring along the transgressive barrier systems on Point Pelee’s eastern shore. It should be noted that these historical records also include human impacts in the region including planting trees on EB to mitigate erosion in the 1880s, marsh drainage schemes beginning in the 1890s, construction of Wheatley Harbor in the 1900s and jetty in the 1950s, and rock armoring of HB and Marentette Beach (located north of EB) following the 1970s (Battin and Nelson, 1978; Baird et al., 2007). Results indicate that longer term transgression rates at EB and HB barriers have exceeded 1 m/y, although short term acceleration or deceleration of shoreline retreat and progradation are observed during cycles of lake level rise and fall. Breaches formed periodically at EB and HB during periods of high lake levels. Breaches may close quickly after initiation (~0–2 years) with limited long-term effects on the barrier, including sediment ridges, overwash fans, and change in barrier width. Significant landward sediment accumulation through storm-induced overwash deposits occur on the lagoonal or pond margin if the breaches remain open for multiple years.

In marine systems, flood tide deltas are common in micro-tidal environments and are composed of a series of landward oriented bedforms and landforms that are formed and maintained by tidal currents (Hayes, 1980). Following the initiation of ‘temporary’ breaches during storm events, storm-induced flood deltas can transfer large volumes of sediment towards the lagoonal margin that can lead to the barrier doubling in width (Armon and McCann, 1979; Leatherman, 1979). The Great Lakes are non-tidal but episodic water level variations can mimic some of the processes responsible for delta development. For example, seiches may cause daily fluctuations of more than 0.2 m across Lake Erie (Trebitz, 2006), equivalent to a micro-tidal diurnal cycle. Davidson-Arnott and Reid (1994) measured alternating flow in and out of a barrier inlet with a periodicity ranging between 12 and 14 minutes. The authors observed that the oscillatory flow initiated bi-directional sediment transport and produced low subaqueous dunes that migrated in and out of the inlet. While these hydrological processes may contribute to the maintenance of breach channels or delta deposits, the role of hourly wind set-up and seiches or seasonal water level fluctuations on lacustrine barriers and breach and recovery processes requires further study.

Given the general fetch limited and low energy environment of Lake Erie, breaches may fill-in and close even during high lake levels, as was observed at EB in 2020. Breaches will typically close as lake levels fall and storm-induced sediment deposits accumulated landward of the former breach, and fill-in of the lakeward shoreline, can significantly increase the barrier width in these locations. During subsequent lake level rise, areas around the former breach are more resilient to subsequent breaching and the process usually migrated to a narrower section of the barrier. Despite the relatively consistent barrier dynamics observed between study sites, the recovery of the expanded breach at HB during the latest peak in lake levels may be further influenced by limited sediment supply due to shoreline armoring on the southern end of the barrier.

Additionally, vertical erosion of the nearshore sediment platform has been recorded by up to -2 m between 1954 and 2019, with continual downcutting occurring out to ~500 m offshore of the current shoreline (Zuzek, 2021). A sediment deficit and potential for higher wave energy reaching the shoreline may have contributed to the rapid breach expansion at HB and could increase the risk of overwash and breaching during storm events. While this requires further investigation, results presented in this study indicate that rates of barrier transgression and breach initiation and recovery histories are highly influenced by decadal lake level highs and lows.

Davidson-Arnott and Fisher (1992) also noted how decadal lake level highs and lows influenced overwash dynamics occurring at Long Point spit, located on the northeastern shoreline of Lake Erie. The authors proposed a conceptual model to indicate the spit's vulnerability to overwash processes and potential for recovery that coincided with rising, peaking, falling, and passive or low lake level phases. In general, the potential for landward transport of sediment through overwash fans or terraces increased as lake levels neared peaks in the cycle. As lake levels neared lows in the cycle, the potential for foredune, beach, and vegetation recovery increased. It is also noted that breaches and landward deposits formed during high lake levels, however, these features often closed quickly and were only a minor source of landward sediment transport relative to overwash and aeolian processes. Modifying the Davidson-Arnott and Fisher (1992) model, a model is proposed that synthesizes the observations of transgressive beach-ridge barrier and breach initiation and recovery processes on the eastern shore of Point Pelee in response to decadal water level cycles (Figure 23):

- 1. Peaking Phase (PP)** – Lake levels are at or near decadal highs and the barrier experiences its highest rates of landward transgression. The overall barrier width is at a minimum and is highly vulnerable to overwashing and breach initiation and/or expansion,

although breach closure may occur due to accumulation of sediment from storm-induced deposits and fill-in during higher energy wave and onshore transport events. Reduction in vegetation cover occurs in areas of disturbances through direct mechanical removal by waves or through burial by overwash deposits above a species tolerance level.

2. Falling Phase (FP) – Lake levels are falling from a Peaking Phase (PP) and are near decadal averages. The barrier width begins to increase, the potential for overwash decreases, and small-scale breaching may occur but will often close quickly. Larger breaches formed during the PP are closed with the barrier increasing in width on the lagoonal or pond margin through storm-induced flood delta deposits. On the lake side, the breach can cause the adjacent shoreline to migrate further landward than the rest of the barrier forming an alongshore concavity or sediment sink. Shoreline transgression rates are usually above longer-term averages but progradation can occur, particularly lakeward of the former breach. Areas of previous disturbances remain largely unvegetated.

3. Stabilizing Phase (SP) – Lake levels are below decadal averages and remain relatively stable near decadal lows. Barrier width is at a maximum and overwash or breaching is highly unlikely to occur. The overall shoreline straightens as sediment is redistributed alongshore and shoreline concavities near former breaches are filled in. Through both the landward expansion from storm-induced flood deposits and shoreline progradation, breaches fully recover and can become the widest section of the barrier. Overall transgression rates are normally below longer-term averages or slightly prograding. Exogenic stress is limited, and vegetation colonization increases in areas of previous disturbances.

4. Rising Phase (RP) – Lake levels are rising from a Stabilizing Phase (SP), or in some cases a shorter period Falling Phase (FP), and are near decadal averages. The barrier is narrowing and the potential for overwash and small-scale breaching increases. Barrier transgression rates typically begin to accelerate and are above longer-term averages. However, following a prolonged SP a lag in acceleration of shoreline retreat can occur and may result from increased sediment accumulation in the nearshore. If occurring after a SP, vegetation is nearing its maximum coverage although new disturbances can cause localized vegetation burial or removal.

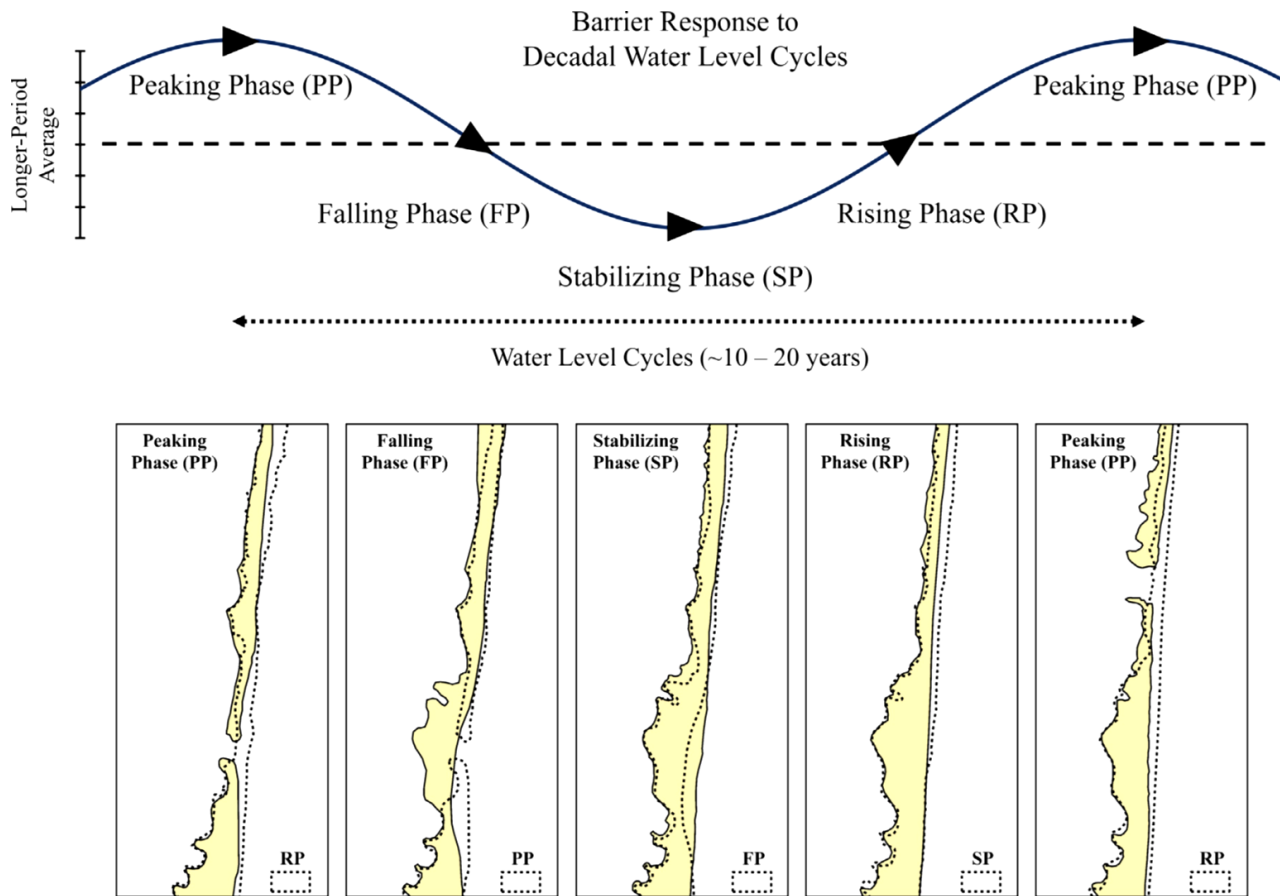


Figure 23: Conceptual model to describe transgressive beach-ridge and breach initiation and recovery processes occurring along Point Pelee’s eastern barriers in response to decadal water level cycles.

While additional research and improvement of the observational record are required to further quantify barrier dynamics, this model can be used to estimate future barrier change in response to decadal lake level cycles, to analyze human impacts including shoreline armoring, to assess the vulnerability of sensitive marsh ecosystems, and to guide further geophysical surveys to reconstruct the history of shoreline transgression along these or other lacustrine barriers. It also serves as a baseline that can be further tested and expanded upon to include other significant system drivers including hourly or seasonal lake level fluctuations, storm frequency and magnitude, and lake ice coverage.

6.3 Conclusion

From the integration of historical aerial images between 1931 and 2020 and in-situ UAV and bathymetric surveys in 2020, barrier beach and breach dynamics occurring on the eastern shore of Point Pelee were examined. While there are several gaps in the time series, findings suggest that barrier transgression, overwash, breach initiation and recovery, and vegetation cover are highly affected by decadal water level cycles relative to longer-term averages. It should be noted that higher frequency lake level fluctuations such as hourly wind set-up or seiches and seasonal variability associated with regional snow melt or evaporation may also influence the barrier dynamics described in this study and requires further investigation as the observational record continues to improve. Furthermore, the formation of breaches were found to be a significant source of landward sediment transport and may represent a self-reinforcing cycle that promotes breach fill-in processes and increases the barrier width and resiliency in response to further lake level fluctuations. Areas of the shoreline that have been stabilized by rock armor following the 1970s may further alter the system dynamics as they are becoming increasingly separated from the transgressive barrier and will be the focus of future monitoring studies.

7. Breach Recovery at Hillman Beach and East Beach

7.1 Results

Over the two-year period of this study, water levels varied between 174.7 m and 174.9 m, following a trend of steady increase since the turn of the century. Water levels in 2020 averaged at 174.9 m, with a minimum of 174.7 m reached in November, and a maximum of 175.1 m set in June. Annual Maximum Ice Cover (AMIC) for this period was 15.9%, a record low that hasn't been observed in almost a decade, when AMIC was 13.9% in 2012. Water levels dropped in the following year, averaging at 174.7 m, with a minimum of 174.6 m in February and March, and a maximum of 174.8 m set in July. The AMIC increased to 85.7% in 2021, strengthening the shoreline protective properties of lake ice. The elevated water levels and lower ice cover in 2020 resulted in larger scale breaching of East Beach in 2020, as compared to 2021. The most prevalent storm events of 2020 occurred on October 11th and November 15th, with peak wave heights reaching 2.12 m and 2.65 m, respectively. In the following year, the main storm events occurred on September 22nd and October 25th, with peak wave heights at 2.55 m and 2.24 m, respectively. When plotted over time by water level, both HB and EB exhibited a different response to the observed changes in water level, lake ice cover, and storm events.

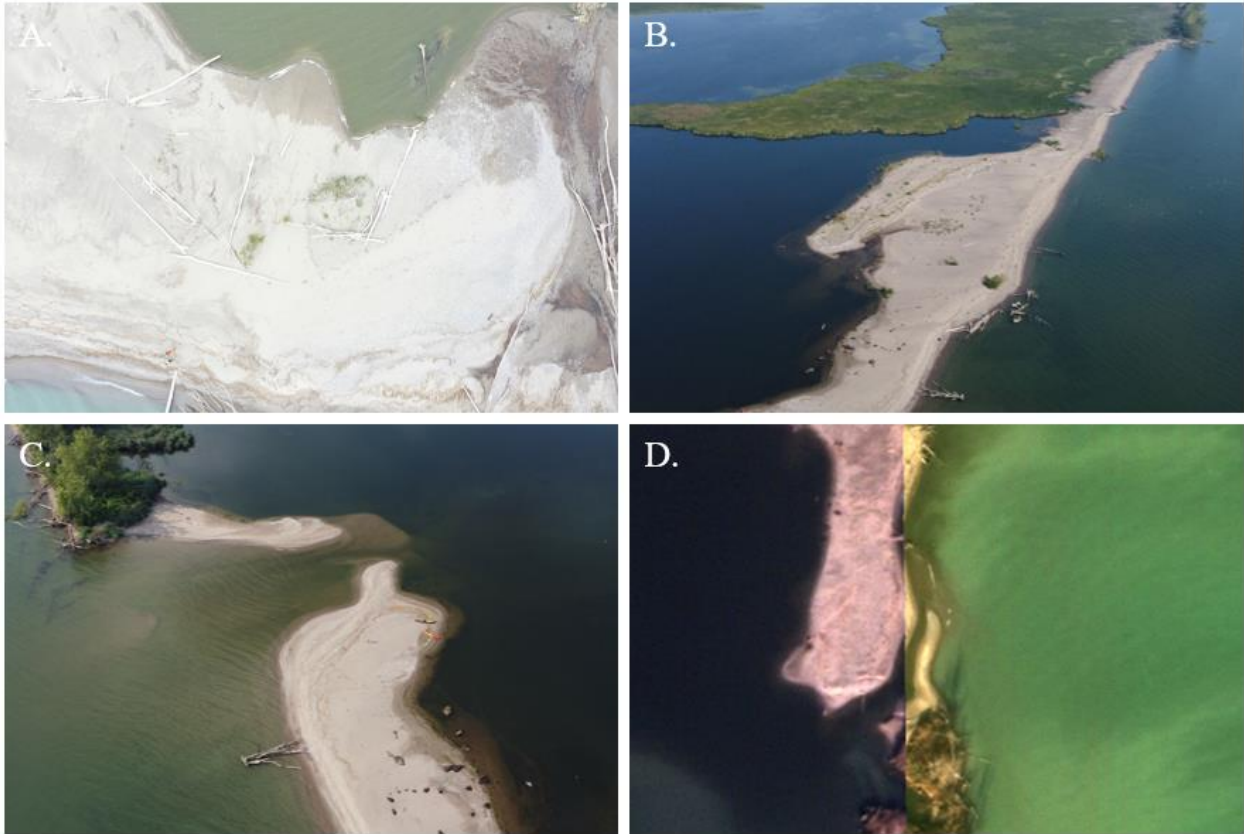


Figure 24: (A) In June 2021, EB had sparse vegetation cover, and (B) 43% of the barrier had doubled in width due to lower water levels exposing sand that was deposited during previous overwash events. (C) In August 2021, breach width decreased to 15 m, both spits were rotating inwards, and the northern spit had a temporary extension from a period of weak currents that allowed for more sedimentation to occur. (D) In November 2021, breach width decreased to 9 m, and multiple overwash fans are visible along the barrier.

7.1.1 East Beach (EB)

The breach at EB was reported closed in November 2020 by staff at Point Pelee National Park and reopened in March 2021 with an initial width of 23 m (aerial imagery provided by Essex Geocortex Database). By June 2021, the breach increased in width to 60 m and was located on the southern end of the barrier, making the southern spit 50 m in length, compared to the northern spit that was approximately 275 m in length. The southern spit was rotating inwards towards the marsh, at roughly a 45-degree angle, due to wave-driven transport. The barrier as a whole has retreated closer to the marsh than it used to be, and sediment transport is visible under water. At this time,

the barrier had sparse vegetation cover (35%) (Figure 24A), and almost half of the barrier has doubled in width due to lower water levels exposing sediment that was deposited during previous overwash events (original width 34 m, 43% of barrier now 82 m) (Figure 24B, 27A). As water levels continued to drop, the breach decreased to 15 m in width by August 2021. The southern spit continued to rotate inwards and was almost perpendicular to the original shoreline location, and the northern spit turned inwards towards the marsh by roughly 45 degrees, decreasing the size of the breach by 45 m. By August 2021, the northern spit was showing patterns of overwash, and had a temporary spit extension from a period of weak currents that allowed for more sedimentation to occur (Figure 24C). In November 2021, water levels dropped by 0.26 m, and the breach width decreased to 9 m such that only a narrow channel was still open (Figure 24D). At this point, multiple overwash fans are visible along the barrier (Figure 27B), suggesting high water levels and larger waves transport and deposit sand across the barrier.

The breach remained open as winter ice formed, and its closure was confirmed by researchers at Point Pelee National Park on June 3rd, 2022 (Figure 25). Lake Erie's monthly average for June was 174.68 m, and 174.66 m specifically on June 3rd. Results from Chapter One and Chapter Two show a consistent loop pattern, on both a large scale and small scale (Figure 26).



Figure 25: The East Beach breach was reported closed by Point Pelee National Park on June 3rd, 2022.

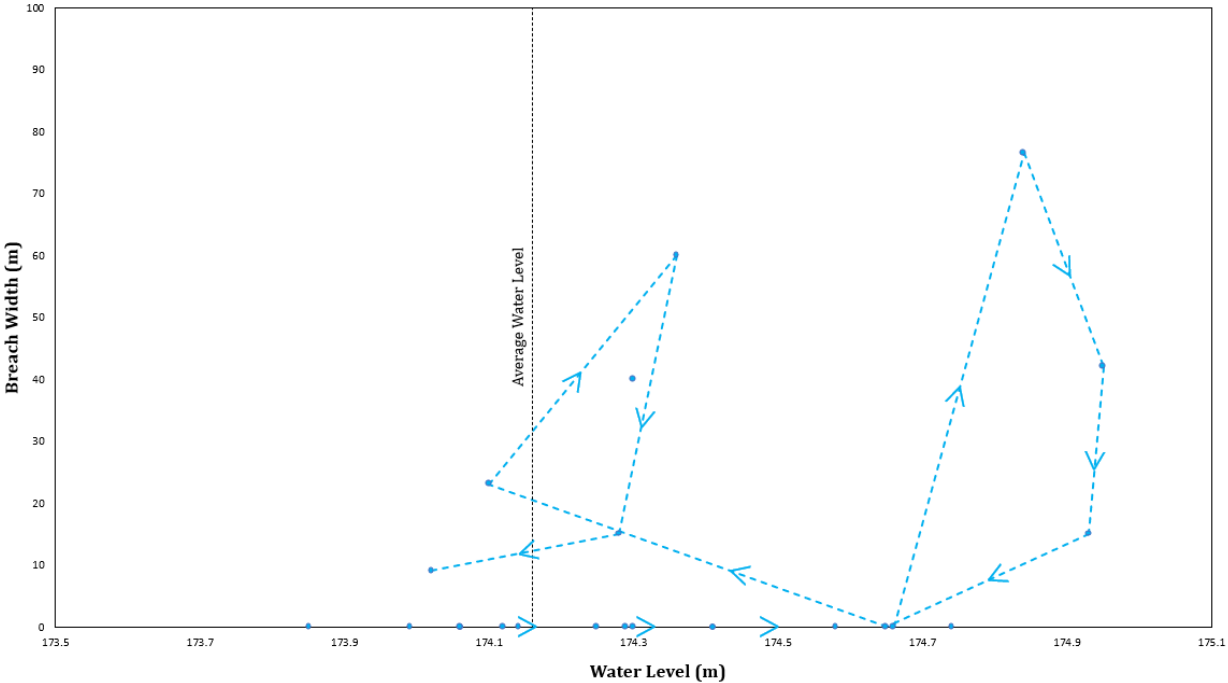


Figure 26: Breach widths at EB plotted against water levels. Loop on the right represents breaching event from Chapter One, and loop on the left represents breaching event from Chapter Two. Data in Table 3.

Table 3: Available historical imagery and supplementary UAV surveys taken during this study alongside water level and breach width at EB. Data represented in Figure 26.

Year	Water Level (m)	Breach Width (m)
1931	173.71	0
1959	173.85	0
1973	174.74	0
1977	174.3	0
1985	174.3	40
1990	174.29	0
2000	173.99	0
2004	174.12	0
2006	174.14	0
2010	174.25	0
2013	174.06	0
2015	174.06	0
2016	174.41	0
2017	174.58	0
2018	174.66	0
2019	174.84	76.5
Mar-20	174.95	42
Aug-20	174.93	15
Nov-20	174.65	0
Mar-21	174.1	23
Jun-21	174.36	60
Aug-21	174.28	15
Nov-21	174.02	9
Jun-22	174.66	0

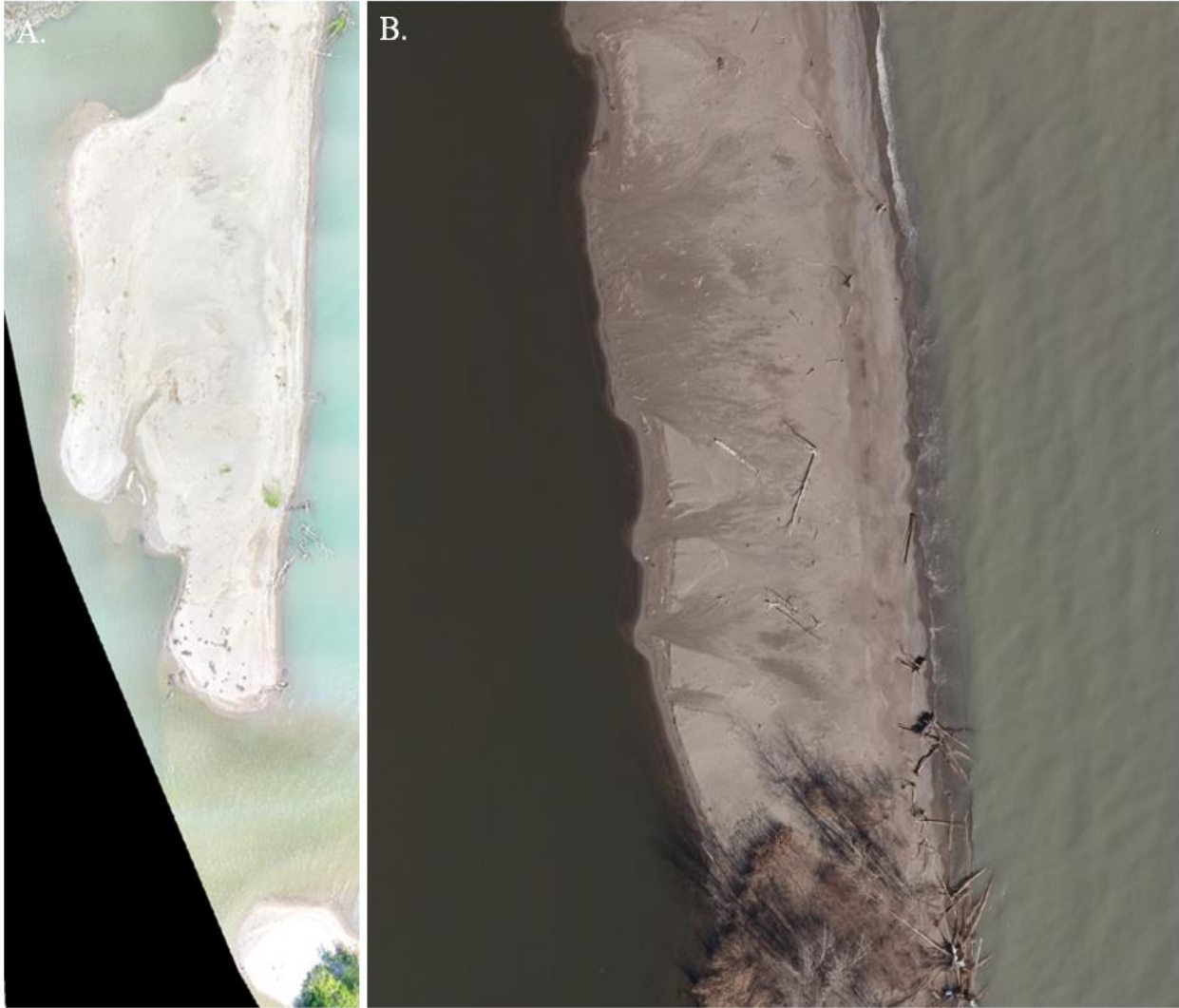


Figure 27: (A) Exposed sediment deposited during overwash events has increased the width of EB barrier by 43%. (B) Survey imagery from November 2021, multiple overwash fans are visible along the barrier.

7.1.2 Hillman Beach (HB)

The breach at HB was first recorded in November 2020 at 299 m wide. This was the last recorded width before the winter, which had an Annual Maximum Ice Cover of 85.7%. In March 2021, it decreased in width to 270 m while water levels were at 174.1 m, a 0.55 m decrease from November 2020. The southern spit of the barrier started to curve inwards towards the marsh and retreated. Both the northern and southern spit were barren but had ample debris from overwash and fallen trees as a result of the retreating shoreline (Figure 28, 29B). Prior to this there were

more trees that extended from the opposite sides of the beach, coming in from the marsh area. In July 2021, the breach increased to 305 m wide as water levels increased by 0.25 m. The northern spit has remained the same, but the southern spit has retreated even further and is only 15 m long, it is separated from the rock revetment (previously the barrier) by a narrow channel of water (Figure 29C). After the survey in November 2021, the breach was recorded to be 277 m wide and water levels dropped down to 174.02 m (Figure 29D). HB appeared to have the potential to follow a similar pattern to EB when the breach width slightly dropped, and because both sites are exposed to the same water levels and wave action. However, once the rock revetement was installed, the breach did not decrease at nearly the same rate it opened, leading to an opposite pattern known as a hysteresis loop (Figure 30).



Figure 28: (A) Treeline at HB, before the rock revetment was installed, in September 2020. (B) Fallen trees and woody debris as a result of the retreating shoreline.

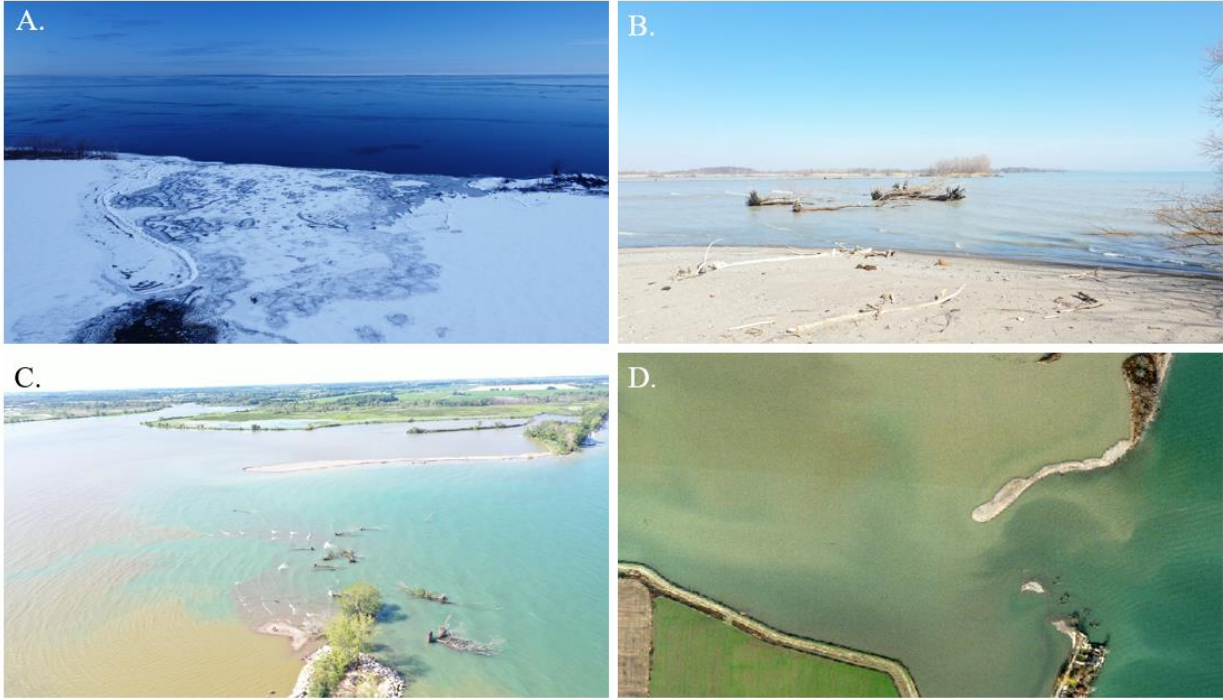


Figure 29: (A) Ice cover at HB on January 25, 2022. (B) Submerged vegetation at HB, due to the retreating shoreline. (C) July 2021, southern spit is separated from the barrier and rock revetement by a channel of water. (D) HB survey from November 2021 (Essex Geocortex Database).

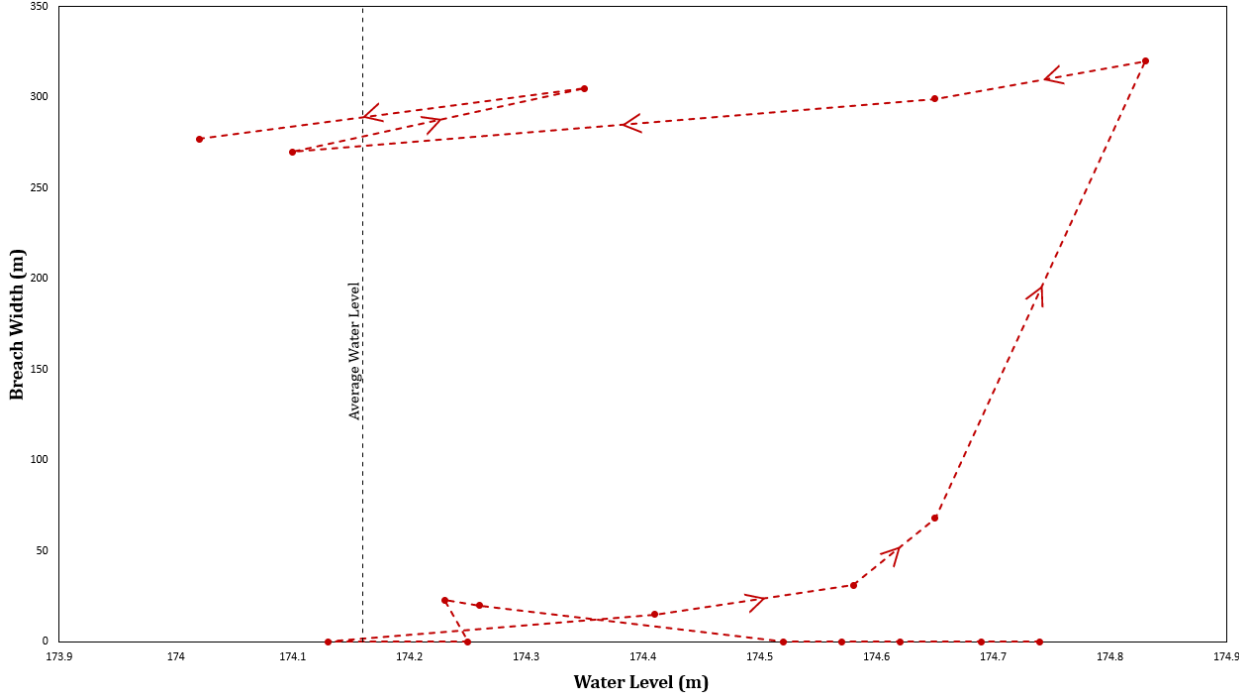


Figure 30: Breach widths at HB plotted against water levels. Breach opens quickly due to the limited sediment supply, and rock revetement is installed right after peak breach width. Data in Table 4.

Table 4: Available historical imagery and supplementary UAV surveys taken during this study alongside water level and breach width at HB. Data represented in Figure 30.

Year	Water Level	Breach Width
1973	174.74	0
1974	174.69	0
1975	174.62	0
1976	174.57	0
1980	174.52	0
1988	174.26	20
1989	174.23	23
2009	174.25	0
2012	174.13	0
2016	174.41	15
2017	174.58	31
Mar-19	174.65	68
Sep-20	174.83	320
Nov-20	174.65	299
Mar-21	174.1	270
Jul-21	174.35	305
Nov-21	174.02	277

7.2 Discussion

The stability of a breach is dependent on the consistency of strong waves and the strength of the longshore transport (Kraus, 2003). In this study, alongside the aforementioned drivers, water levels are considered to play a main role in barrier breaching in lacustrine environments. Water levels are the control on longshore transport and the waves impacting the barrier. At EB, barrier initiation and closure have been found to follow a four-step cycle of breaching (Figure 31, 32):

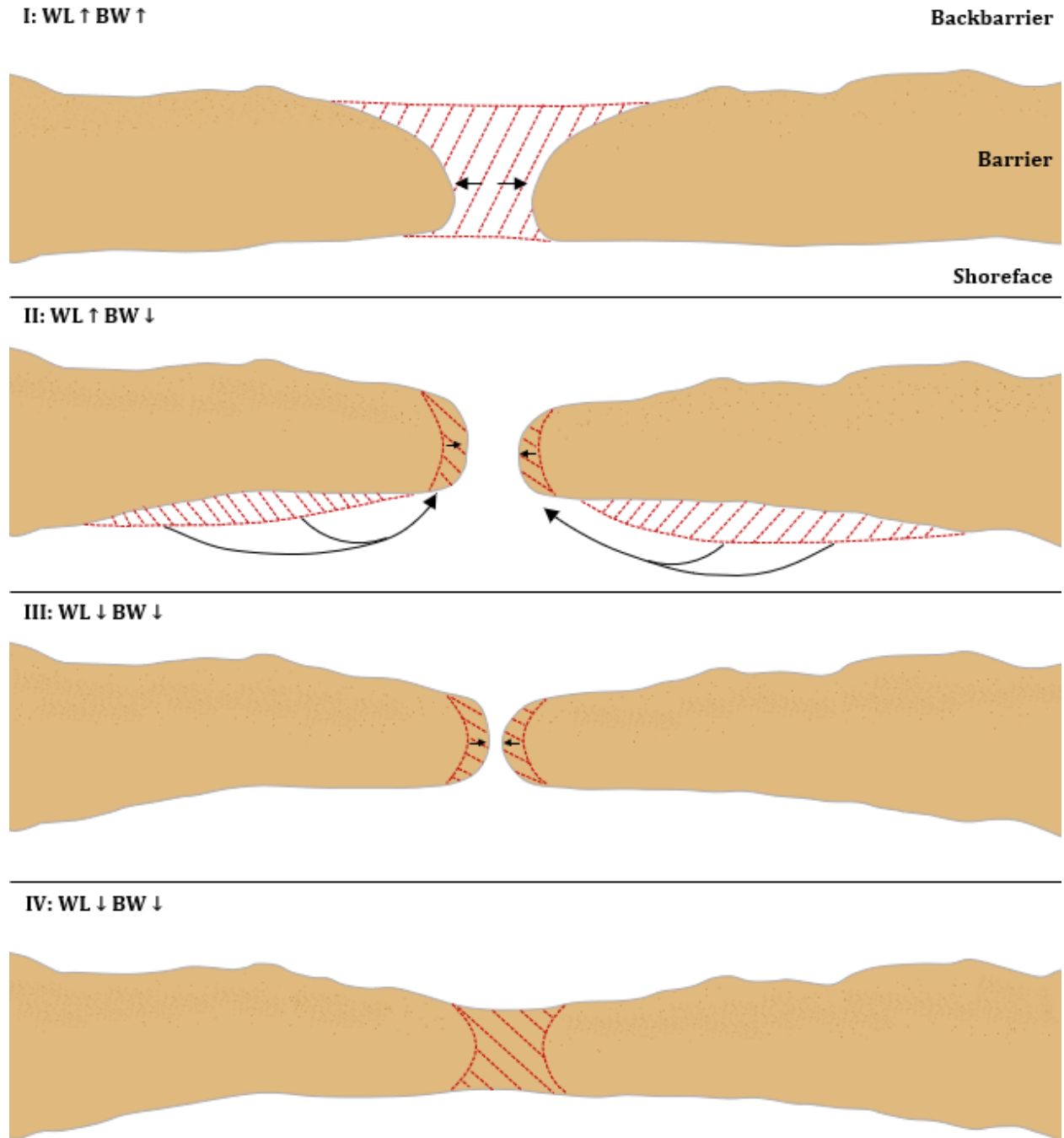


Figure 31: Four-step cycle of barrier breaching of a shoreline with no coastal structures and adequate sediment supply. (I) Large increase in lake water levels causes the barrier beach to breach in the middle of the barrier. (II) Increased wave action erodes sediment from sides of barrier and is then carried to the centre, decreasing breach width. (III) Water levels drop, exposing low elevation of the breach. (IV) Further drop in water levels fully closes the beach.

I) Large increase in lake water levels that exceeds the elevation of the barrier beach causes it to breach in the middle of the barrier, at the weakest point. At this point, barrier elevation is the lowest, width is the narrowest, and vegetation is sparse or non-existent. At EB this occurred at lake levels of 174.84 m, and a breach width of 76.5 m.

II) Further increase in lake water levels, with a small decrease in breach width. As water levels continue to increase during this step, increased wave action erodes sediment away from the stronger sides of the barrier where elevation is high. Through alongshore transport, this sediment is carried to the centre of the barrier, slightly beginning to fill in the breach. At EB, this was observed when there was a 0.11 m increase in lake water level, but the breach decreased to 42 m wide.

III) Decrease in lake water levels, and further decrease in breach width. The breached part of the barrier has a naturally low elevation, therefore when water levels begin to drop, the sand becomes exposed again. At EB, the breach drastically decreases to 15 m wide after merely a 0.08 m drop in water level.

IV) Decrease in lake water levels (0.28 m) causes the breach to close.

The ability of a barrier beach to fully recover after breaching relies on its ability to recover in width and elevation prior to the next storm event or period of water level rise. Historically, EB has exceeded the water levels that caused it to breach in 2019, but while in the recovery phase following the first breaching event, the barrier became vulnerable to breaching at lower water levels (Figure 26).

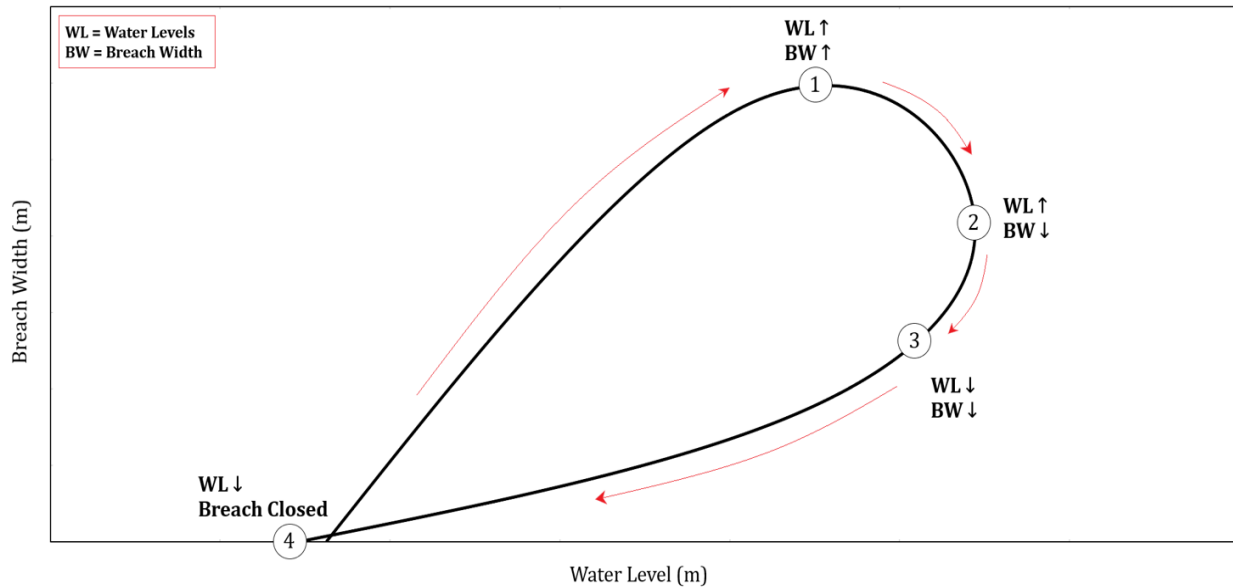


Figure 32: Conceptual model visualizing barrier breaching of a shoreline with no coastal structures and adequate sediment supply.

It is reasonable to expect that under natural circumstances (a barrier beach without adjacent coastal structures) HB would also follow this cycle. However, after a revetment was put in place, the rate of growth is much faster than the rate at which the breach closes (Figure 34). The patterns of barrier breaching at HB show a trend identified as a hysteresis loop. Defined as a time-lag response by Cho, Suzuki & Nakamura (2010), hysteresis is seen in barrier breaching as breach initiation and growth is occurring at a faster rate than breach closure and recovery. HB is a starved system due to the Wheatley Harbour Jetty trapping alongshore sediment transport and the installation of a revetment only starved it further as coastal structures can disrupt longshore drift, cut off sediment supply, and disrupt normal processes of wind, wave, and current movement (Vaidya et al., 2015; Airoidi et al., 2005; Figure 33). Cutting off sediment supply in turn controls barrier inertia (how rapidly a barrier can be reorganized in response to external forces), restricting the response time of a barrier to external forces (Cooper et al., 2018).

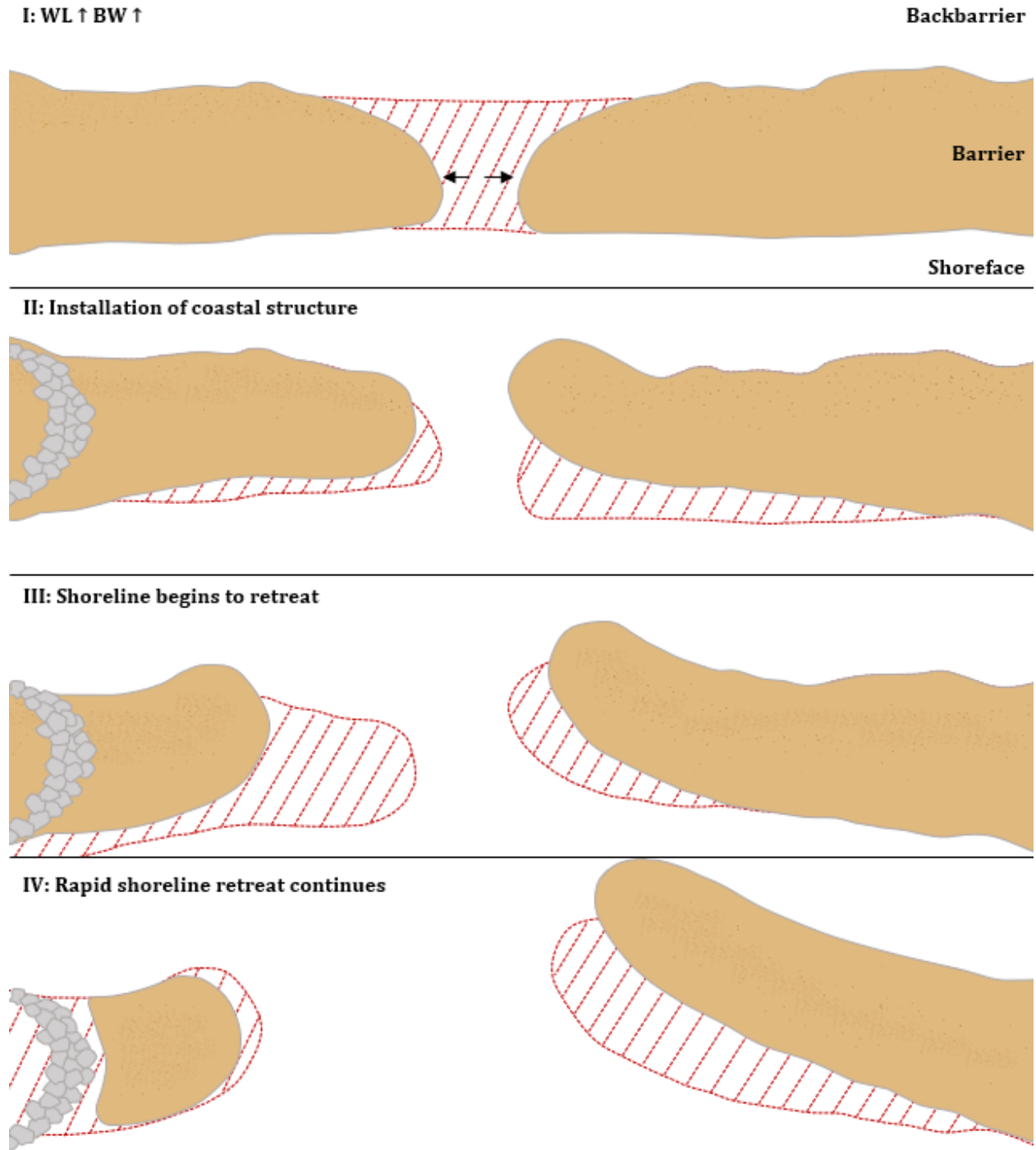


Figure 33: Barrier breaching of a modified shoreline. (I) Increase in water levels cause the barrier beach to breach. (II) Installation of hard coastal structure. (III) Shoreline begins to retreat due to cut off sediment supply. (IV) Rapid shoreline retreat continues; breach expansion occurs at a much faster rate than closure.

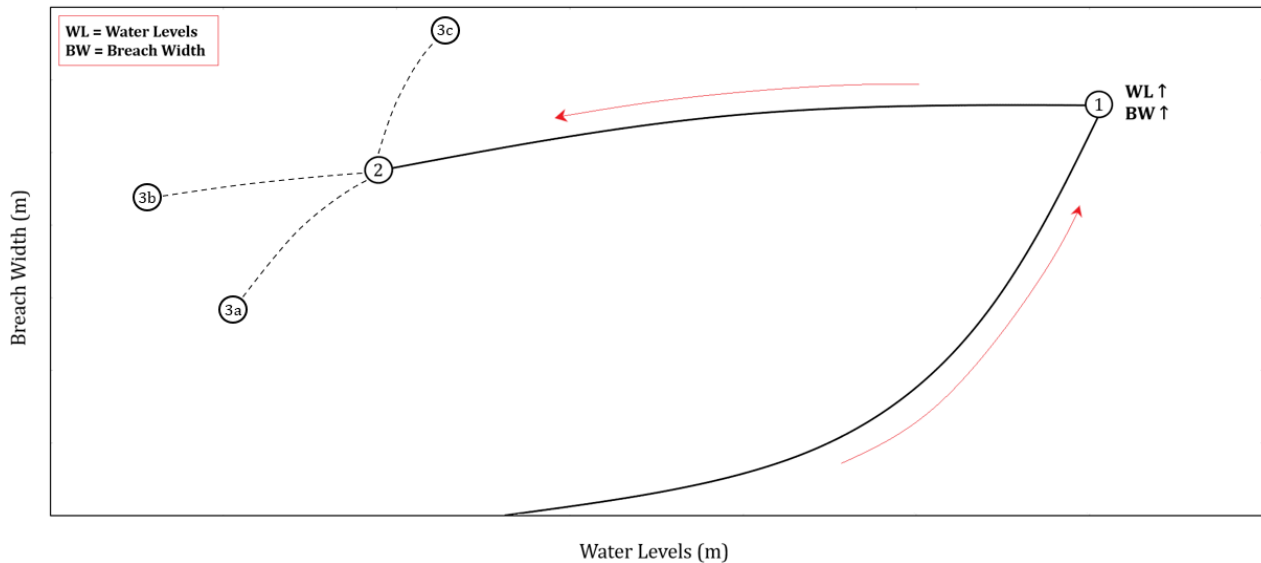


Figure 34: Conceptual model visualizing barrier breaching of a modified shoreline, and three potential future scenarios.

Theuerkauf and Braun (2021) attribute abrupt changes in water levels during storm events as the driving force of erosion and overwash. Climate change in the Great Lakes is projected to increase the variability of water level fluctuations, increasing the frequency and intensity barrier breaching (Theuerkauf and Braun, 2021). While water levels are a driving force, both Hillman Beach and East Beach respond differently to variations in water levels (Figure 35, 36), despite being in close proximity, and this is attributed to sediment supply. EB still has sediment supply coming in from the north and south, along the rest of the eastern shoreline of Point Pelee, and through offshore currents (potentially sand bars). EB is a self-healing coastal system due to an adequate amount of sediment supply, HB is a permanent scar that is likely to never recover naturally, unless a significant drop in water levels occur, and will need some form of intervention. During breaching periods at EB, wave action caused the spits to migrate landwards, and after the breach closed, the barrier as a whole was retreated (Figure 37, 38). Due to an inadequate amount of sand at HB, the fate of the breach is completely controlled by water levels, and the small decrease observed this year may be responsible for the slight decrease in breach width. Despite the

future of Hillman Beach being unknown, three potential scenarios can be hypothesized (Figure 34). In the first scenario (3a), water levels drop below the elevation of the breached part of the barrier, sediment is exposed, and the beach slowly starts to repair itself. In the second scenario (3b), water levels drop but due to a lack of sediment, it can not recover to its prior potential. In the third scenario (3c), water levels increase, and the size of the breach increases with it. This study helped bridge the gap in current breaching literature that focused on marine and tidal environments and introduced lacustrine environments.

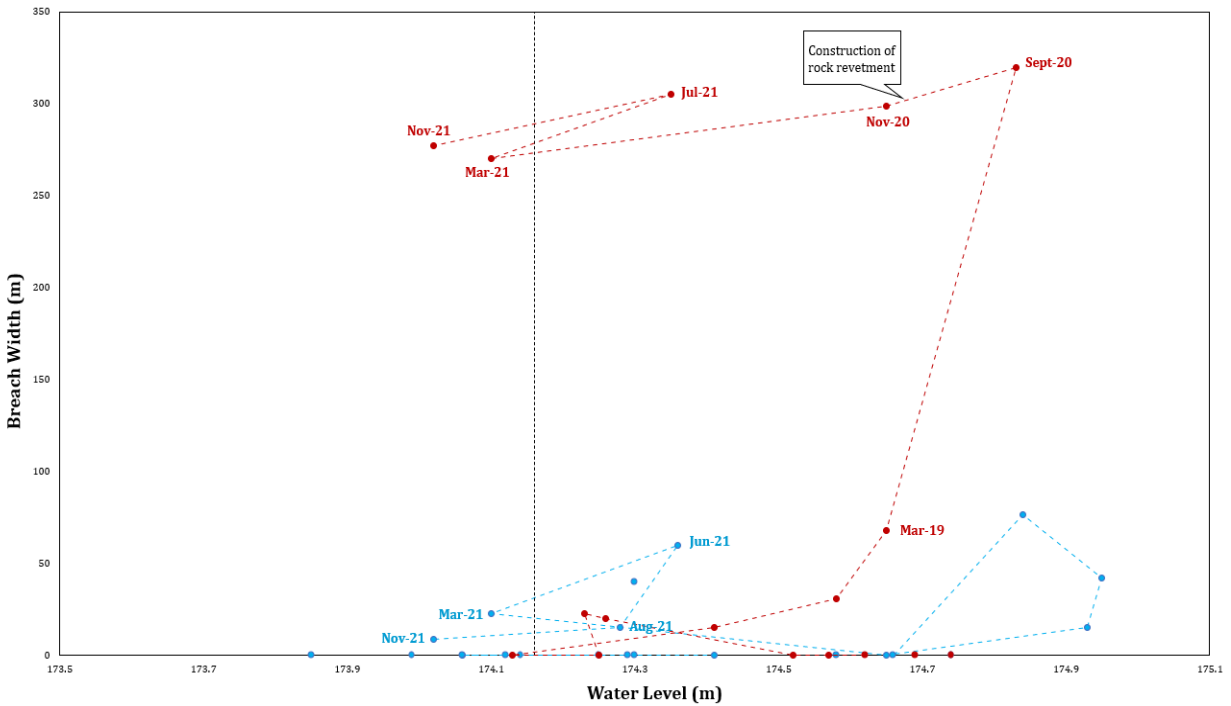


Figure 35: Breach widths plotted against water levels at both EB (blue) and HB (red), displaying much larger scale breaching at HB. Data from Table 3 and 4.

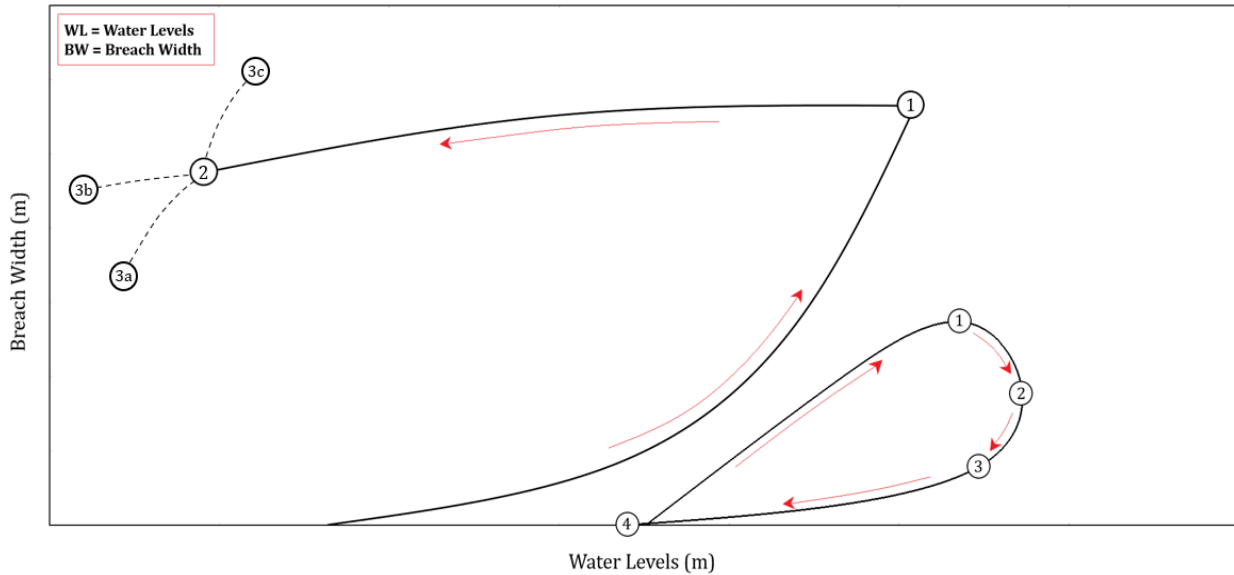


Figure 36: Conceptual model of barrier breaching at an unmodified shoreline with adequate sediment supply, and a modified shoreline with limited sediment supply. Stylized model of Figure 35.

7.3 Conclusion on Breach Recovery

The ability of a barrier to withstand breaching depends on its sediment budget and alongshore transport. Barrier beaches with a steady sediment supply and no obstructions in alongshore transport respond to high water levels and increased wave action in a four-step cycle. When water levels surpass a critical elevation, or waves scour a trough through a barrier, a breach is initiated, and will continue to increase in width as water levels increase. Once the weakest point of a barrier is breached, wave action starts to erode the sides of the barrier – providing sediment to the breach in a self-repairing cycle. The breach closes when it receives enough sediment and/or water levels drop. In the presence of a modified shoreline and limited sediment supply, barriers follow a hysteretic model in which breach initiation occurs at a faster rate than closure and recovery, which will only occur if water levels drop below elevation of breach inlet. Coastal structures cut off sediment supply and rapidly erode the barrier at a rate where natural sediment supply can not repair.



Figure 37: First UAV survey of this project (conducted in August 2020), compared to latest shoreline digitization (survey from July 2022).



Figure 38: Last UAV survey of this project (conducted in July 2022), compared to first shoreline digitization (survey from August 2020).

8. Conclusion and Future Research

This study focused on quantifying historical and modern shoreline retreat alongside breach initiation, expansion, and closure at East Beach (EB) and Hillman Beach (HB), on the Point Pelee Foreland. Lake level fluctuations were examined on a decadal to centennial scale to establish the controls on barrier transgression and breaching. This was done by gathering previously published reports and aerial photographs, digitizing shorelines of every available year in ArcGIS, quantifying retreat by calculating EPR and LRR, and conducting UAV surveys to continue monitoring breaching on a monthly basis to monitor breaching on a smaller scale as historical imagery was only done annually. Previous studies most often studied the initiation of breaches due to tidal events, rather than episodic and storm induced breaching. This project introduced barrier breaching in non-tidal, freshwater environments.

Despite close proximity and experiencing similar water levels, EB and HB have responded differently, this study attributes this difference to sediment supply. EB has steady sediment supply from the north and the south; however HB is starved from the north due to the Wheatley harbour and attached jetty, and from the south as a result of the rock revetement. At EB, barrier initiation and closure have been found to follow a four-step cycle of breaching: 1) A large increase in lake water levels causes the barrier to breach at the weakest point, 2) continuing increase in water levels erodes the sides of the barrier, transporting sediment to the centre, decreasing the width of the breach, 3) decreasing water levels expose lower elevation sediments, decreasing the breach width, and 4) a final decrease in lake levels closes the breach. In the presence of a modified shoreline, such as HB, high water levels or a particularly strong storm event initiate a breach, and weak longshore transport and limited sediment supply prevent it from being able to close.

For future research, continuous monitoring of these two sites is essential to confirm the proposed four-step model. Completing a historical analysis of additional breached barriers around the Great Lakes (Table 1) will further strengthen our understanding of this process. Further research on the removal of hard coastal structures along with the implementation of nature-based solutions can help begin recovery projects at Hillman Beach. Sand nourishment is needed to add more sediment into the budget, after removing hard structures that are trapping sediment. Though it is possible that the HB breach can close, the barrier has migrated and indented in a way that has not been seen anywhere else, and this will prevent it from returning to its old position. Natural breaching has been found to be important to the ecological integrity of Point Pelee, this process can be maintained by increasing the amount of available sediment and slowing down wave energy to ensure breaching does not reach the extreme scenario seen at HB. More numerical modelling on breaching in non-tidal, freshwater environments are needed, including hydrodynamic modelling of inshore and offshore wave movement. Barrier beaches provide essential protection to inshore environments and habitats through wave energy dissipation and protection against storm damage. These environments have become increasingly vulnerable as these services are threatened by climate change. Climate change threatens the existence of Point Pelee (Zuzek, 2021), along with its cultural and ecological significance.

References

- Airoidi, L., Abbiati, M., Beck, M.W., Hawkins, S.J., et al. (2005) An ecological perspective on the deployment and design of low-crested and other hard coastal defence structures. *Coastal Engineering*. [Online] 52 (10-11), 1073–1087. Available from: doi:10.1016/j.coastaleng.2005.09.007.
- Angove, M., Kozlosky, L., Chu, P., Dusek, G., et al. (2021) Addressing the meteotsunami risk in the United States. *Natural Hazards*. [Online] 106 (2), 1467–1487. Available from: doi:10.1007/s11069-020-04499-3.
- Armon, J.W., McCann, S.B., (1979) Morphology and landward sediment transfer in a transgressive barrier island system, southern Gulf of St. Lawrence, Canada. *Marine Geology*, 31 (3-4), 333–344.
- Assel, R., Cronk, K. & Norton, D. (2003) Recent trends in Laurentian Great Lakes Ice cover. *Climatic Change*. [Online] 57 (1/2), 185–204. Available from: doi:10.1023/a:1022140604052.
- BaMasoud, A. & Byrne, M.-L., 2011. Analysis of Shoreline Changes (1959–2004) in Point Pelee National Park, Canada. *Journal of Coastal Research*, 276, pp.839–846.
- Baird, W.F., B. Stephenson, Gartner Lee Limited, Golder Associates, The Outspan Group Inc., Todgham & Case Associates Inc. et l'Université de Guelph, Ridgetown. (2007) Sustainable Management Strategy for Southeast Leamington: Phase 2 Report.
- BaMasoud, A. & Byrne, M.-L., (2012) The impact of low ice cover on shoreline recession: A case study from Western Point Pelee, Canada. *Geomorphology*, 173-174, pp.141–148.
- Battin, J.G., Nelson, J.G., (1978) Man's Impact on Point Pelee National Park. *National and Provincial Parks Association of Canada*. Resource Integrations Systems Ltd., Toronto.
- Basco, D.R. & Shin, C.S., (1999) A One-Dimensional Numerical Model for Storm- Breaching of Barrier Islands. *Journal of Coastal Research*, 15(1), pp.241–260.
- Bechle, A.J. et al., (2016) Meteotsunamis in the Laurentian Great Lakes. *Scientific Reports*, 6(1).
- Boak, E.H., Turner, I.L., (2005) Shoreline definition and detection: a review. *Journal of Coastal Research*, 21 (4 (214)), pp.688–703.
- Brenner, O.T., Moore, L.J. & Murray, A.B. (2015) The complex influences of back-barrier deposition, substrate slope and underlying stratigraphy in barrier island response to sea-level rise: Insights from the Virginia Barrier Islands, Mid-Atlantic Bight, U.S.A. *Geomorphology*. [Online] 246334–350. Available from: doi:10.1016/j.geomorph.2015.06.014.

- Carter, R.W.G. (1988) Effects of Sea Level Change on Shorelines. In: *Coastal Environments: An Introduction to the Physical, Ecological and Cultural Systems of Coastlines*. London, Academic Press Limited. p. 267.
- Coakley, J.P., (1975) The formation and evolution of Point Pelee, Western Lake Erie. *Canadian Journal of Earth Sciences*, 13(1), pp.136–144.
- Coakley, J.P., Crowe, A.S., Huddart, P.A., (1998) Subsurface sediment profiles below Point Pelee: indicators of postglacial evolution in western Lake Erie. *Canadian Journal of Earth Sciences*, 35, pp.88-99.
- Cooper, J.A.G, Green, A.N., Loureiro, C., (2018) Geological constraints on mesoscale coastal barrier behaviour. *Global and Planetary Change*, 168, pp.15-34.
- Danard, M., Munro, A. & Murty, T., (2002) Storm Surge Hazard in Canada. *Natural Hazards*, 28, pp.407–431.
- Davidson-Arnott, R.G. & Fisher, J.D., (1992) Spatial and temporal controls on overwash occurrence on a Great Lakes Barrier Spit. *Canadian Journal of Earth Sciences*, 29(1), pp.102–117.
- Davidson-Arnott, R.G. & Law, M.N., (1996) Measurement and Prediction of Long-Term Sediment Supply to Coastal Foredunes. *Journal of Coastal Research*, 12(3), pp.654–663.
- Davidson-Arnott, R.G. & Reid, H.E. (1994) Sedimentary processes and the evolution of the distal bayside of Long Point, lake erie. *Canadian Journal of Earth Sciences*. [Online] 31 (9), 1461–1473. Available from: doi:10.1139/e94-129.
- Davidson-Arnott, R.G. & Van Heyningen, A.G., (2003) Migration and sedimentology of longshore sandwaves, Long Point, Lake Erie, Canada. *Sedimentology*, 50(6), pp.1123–1137.
- Drezner, T.D., (2019) Vegetation Associations of the endangered *Opuntia cespitosa* (prickly pear, Cactaceae) and microsite variation in Point Pelee National Park, Ontario, Canada. *Physical Geography*, 42(2), pp.126–142.
- Dolan, R., Fenster, M.S., Holme, S.J., (1991) Temporal analysis of shoreline recession and accretion. *Journal of Coastal Research*, 7(3), pp.723–744
- Gharib, J., Smith, A. & Houser, C. (2021) Barrier beaches and breaches: Historical changes on the Point Pelee Foreland. *Journal of Great Lakes Research*. [Online] 47 (6), 1554–1564. Available from: doi:10.1016/j.jglr.2021.06.011.
- Halpenny, E.A., 2006. *Environmental Behaviour, Place Attachment and Park Visitation: A case study of visitors to Point Pelee National Park*. thesis.

- Hamblin, P.F. (1987) Meteorological Forcing and Water Level Fluctuations on Lake Erie. *Journal of Great Lakes Research*. 4 (13), 436–453.
- Harris, L., (2000) Wind Tide and seiches in the Great Lakes. *Coastal Engineering Proceedings*, 1(4), pp.25–45.
- Hartmann, H.C. (1990) Climate change impacts on Laurentian Great Lakes Levels. *Climatic Change*. [Online] 17 (1), 49–67. Available from: doi:10.1007/bf00149000.
- Hayes, M.O., (1980) General morphology and sediment patterns in tidal inlets. *Sedimentary Geology*. 26 (1–3), 139–156.
- Herdendorf, C.E., (1987) The Ecology of the Coastal Marshes of Western Lake Erie: A Community Profile. *National Wetlands Research Center*.
- Hosier, P.E. & Cleary, W.J. (1977) Cyclic geomorphic patterns of washover on a barrier island in southeastern North Carolina. *Environmental Geology*. [Online] 2 (1), 23–31. Available from: doi:10.1007/bf02430662.
- Houser, C., Hapke, C. & Hamilton, S., (2008) Controls on coastal dune morphology, shoreline erosion and barrier island response to extreme storms. *Geomorphology*, 100(3-4), pp.223–240.
- Houser, C. et al., (2018) Role of the Foredune in Controlling Barrier Island Response to Sea Level Rise. In *Barrier Dynamics and Response to Changing Climate*. Cham, Switzerland: Springer International Publishing, pp. 175–207.
- Jacobs, D.M. & Lytwyn, V.P., (2020) Naagan GE Bezhig Emkwaan. *Ontario History*, 112(2), p.191.
- Keough, J.R. et al., (1999) Hydrogeomorphic factors and ecosystem responses in coastal wetlands of the Great Lakes. *Wetlands*, 19(4), pp.821–834.
- Kraus, N.C., Militello, A. & Todoroff, G., (2002) Barrier Breaching Processes and Barrier Spit Breach, Stone Lagoon, California . *Shore & Beach*, 70(4).
- Kraus, N.C. & Wamsley, T.V., (2003) Coastal Barrier Breaching, Part 1: Overview of Breaching Processes. *ERDC/CHL*, CHETN-IV-56.
- Kraus, N.C., (2003) Analytical model of incipient breaching of coastal barriers. *Coastal Engineering Journal*, 45(4), pp.511–531.
- Kraus, N.C. & Hayashi, K., (2005) Numerical morphologic model of barrier island breaching. *Coastal Engineering 2004*, pp.2120–2132.

- Leatherman, S.P., (1979) Barrier dune systems: A reassessment. *Sedimentary Geology*, 24(1-2), pp.1–16.
- Libicki, C. & Bedford, K.W., (1990) Sudden, extreme Lake Erie storm surges and the interaction of wind stress, resonance, and Geometry. *Journal of Great Lakes Research*, 16(3), pp.380–395.
- Linares, A., Wu, C.H., Bechle, A.J., Anderson, Kristovich, D.A.R., (2019) Unexpected rip currents induced by a meteotsunami. *Scientific Reports*.
- Lofgren, B.M., Quinn, F.H., Clites, A.H., Assel, R.A., et al. (2002) Evaluation of potential impacts on Great Lakes water resources based on climate scenarios of two GCMs. *Journal of Great Lakes Research*. [Online] 28 (4), 537–554. Available from: doi:10.1016/S0380-1330(02)70604-7.
- MacArthur, R.H. & Wilson, E.O. (1967) In: *The Theory of Island Biogeography*. Princeton, N.J., Princeton University Press.
- Malm, J., Bengtsson, L., Terzhevik, A., Boyarinov, P., et al. (1998) Field study on currents in a shallow, ice-covered Lake. *Limnology and Oceanography*. [Online] 43 (7), 1669–1679. Available from: doi:10.4319/lo.1998.43.7.1669. Mamo, L.T., Dwyer, P.G., Coleman, M.A., Dengate, C., et al. (2022) Beyond Coastal Protection: A robust approach to enhance environmental and social outcomes of coastal adaptation. *Ocean & Coastal Management*. [Online] 217106007. Available from: doi:10.1016/j.ocecoaman.2021.106007.
- Mattheus, C.R., Fowler, J.K., Diggins, J.P., Allen, D.F., (2016) Barrier-spit geomorphology and inlet dynamics in absence of tides: Evolution of the north pond system, eastern Lake Ontario, New York State. *Earth Surface Processes and Landforms*, 41(10), pp.1386–1398.
- Meadows, G.A., Meadows, L.A., Wood, W.L., Hubertz, J.M., et al. (1997) The relationship between Great Lakes water levels, wave energies, and Shoreline Damage. *Bulletin of the American Meteorological Society*. [Online] 78 (4), 675–682. Available from: doi:10.1175/1520-0477(1997)078<0675:trbglw>2.0.co;2.
- Mercer, D., Sheng, J., Greatbatch, R.J., Bobanovic, J., (2002) Barotropic waves generated by storms moving rapidly over shallow water. *Journal of Geophysical Research*, 107(C10).
- Monserrat, S., Ibbetson, A. & Thorpe, A.J., (1991) Atmospheric gravity waves and the ‘rissaga’ phenomenon. *Quarterly Journal of the Royal Meteorological Society*, 117(499), pp.553–570.
- Morton, R.A., (1978) Large-scale rhomboid bed forms and sedimentary structures associated with Hurricane Washover*. *Sedimentology*, 25(2), pp.183–204.
- Orescanin, M.M, Scooler, J., (2018) Observations of episodic breaching and closure at an ephemeral river. *Continental Shelf Research*, 166, pp.77-82.

- Orford, J.D., Carter, R.W.G., McKenna, J. & Jennings, S.C. (1995) The relationship between the rate of mesoscale sea-level rise and the rate of retreat of swash-aligned gravel-dominated barriers. *Marine Geology*. [Online] 124 (1-4), 177–186. Available from: doi:10.1016/0025-3227(95)00039-2.
- Orford, J.D., Forbes, D.L. & Jennings, S.C. (2002) Organisational controls, typologies and time scales of paraglacial gravel-dominated coastal systems. *Geomorphology*. [Online] 48 (1-3), 51–85. Available from: doi:10.1016/s0169-555x(02)00175-7.
- Otvos, E.G. (2012) Coastal barriers — nomenclature, processes, and classification issues. *Geomorphology*. [Online] 139-14039–52. Available from: doi:10.1016/j.geomorph.2011.10.037.
- Pierce, J.W., (1970) Tidal inlets and Washover fans. *The Journal of Geology*, 78(2), pp.230–234.
- Plant, N.G. & Stockdon, H.F., (2012) Probabilistic prediction of barrier-island response to Hurricanes. *Journal of Geophysical Research: Earth Surface*, 117(F3).
- Porterfield, J. (2021) *High Wave Events on the Great Lakes in Relation to El Niño-Southern Oscillation Influences on Mid-Latitude Cyclones: What Can Storm Patterns Tell Us about Extreme Wave Events in the Future?*. thesis.
- Quinn, F.H., (2002) Secular changes in Great Lakes water level seasonal cycles. *Journal of Great Lakes Research*, 28(3), pp.451–465.
- Safak, I., J. C. Warner, J. H. List, (2016) Barrier island breach evolution: Alongshore transport and bay-ocean pressure gradient interactions. *Journal of Geophysical Research: Oceans*, 121, 8720– 8730, doi:10.1002/2016JC012029
- Sallenger, A.H., (2000) Storm Impact Scale for Barrier Islands. *Journal of Coastal Research*, 16(3).
- Schwab, W.C., Thieler, E.R., Allen, J.R., Foster, D.S., et al. (2000) Influence of Inner-Continental Shelf Geologic Framework on the Evolution and Behavior of the Barrier-Island System between Fire Island Inlet and Shinnecock Inlet, Long Island, New York. *Journal of Coastal Research*. 16 (2), 408–422.
- Smith, A. & Houser, C. (In Review.) Perspectives on Great Lakes Coastal Management: A Case Study of the Point Pelee Foreland, Canada. *Ocean and Coastal Management*.
- Smith, G. & Zarillo, G., (1988) Short-Term Interactions Between Hydraulics and Morphodynamics of a Small Tidal Inlet, Long Island, New York. *Journal of Coastal Research*, 4(2), pp.301–314.

- Sogut, D., Farhadzadeh, A. & Jensen, R.E. (2018) Characterizing the great lakes marine renewable energy resources: Lake michigan surge and wave characteristics. *Energy*. [Online] 150781–796. Available from: doi:10.1016/j.energy.2018.03.031.
- Surette, H.J. (2006) *Processes influencing temporal variation in fish species composition in Point Pelee National Park*. thesis.
- Suter, J.R, Nummedal, D., Maynard, A.K., Kemp, P., (1982) A Process-Response Model for Hurricane Washover. *Coastal Engineering*.
- Tanaka, K., (2010) Atmospheric pressure-wave bands around a cold front resulted in a meteotsunami in the East China Sea in February 2009. *Natural Hazards and Earth System Sciences*, 10(12), pp.2599–2610.
- Theuerkauf, E.J. & Braun, K.N. (2021) Rapid water level rise drives unprecedented coastal habitat loss along the Great Lakes of North America. *Journal of Great Lakes Research*. [Online] 47 (4), 945–954. Available from: doi:10.1016/j.jglr.2021.05.004.
- Trebitz, A.S., (2006) Characterizing Seiche and tide-driven daily water level fluctuations affecting coastal ecosystems of the Great Lakes. *Journal of Great Lakes Research*, 32(1), pp.102–116.
- Trenhaile, A.S. & Dumala, R., (1978) The geomorphology and origin of Point Pelee, Southwestern Ontario. *Canadian Journal of Earth Sciences*, 15(6), pp.963–970.
- Trenhaile, A.S., Pepper, D.A., Trenhaile, R.W., Dalimonte, M., (1998) Canadian Landform Examples - 35. *Canadian Geographer*, 42(1), pp.94–99.
- U.S. Army Engineer District, (1968) Report on Hurricane "Beulah". *Corps of Engineers Galveston, Texas*.
- Vaidya, A.M., Kori, S.K. & Kudale, M.D. (2015) Shoreline Response to Coastal Structures. *Aquatic Procedia*. 4333–340.
- Wamsley, T.V. & Kraus, N.C., (2003) Coastal Barrier Island Breaching, Part 2: Mechanical Breaching and Breach Closure. *ERDC/CHL, CHETN-IV-56*.
- Wernette, P. & Weymer, B.A., (2017) Scale-dependent behavior of the foredune: Implications for barrier island response to storms and sea-level rise. *Geomorphology*, 303, pp.362–374.
- Wernette, P. et al., (2018) Influence of a spatially complex framework geology on Barrier Island Geomorphology. *Marine Geology*, 398, pp.151–162.
- Young, G.C. & Potter, I.C. (2003) Influence of an artificial entrance channel on the ichthyofauna of a large estuary. *Marine Biology*. [Online] 142 (6), 1181–1194. Available from: doi:10.1007/s00227-003-1012-0.

Zuzek, P.J., (2021) Southeast Leamington Graduated Risk Floodplain Mapping Project. Prepared for the Municipality of Leamington.

Appendix

Table 5: Minimum barrier width, maximum barrier width, and average barrier width for each available year at East Beach.

Year	Minimum Barrier Width (m)	Maximum Barrier Width (m)	Average Barrier Width (m)
1931	79.60	177.51	117.02
1959	45.88	155.54	87.82
1973	44.47	153.99	82.03
1977	31.96	130.20	66.70
1985	10.03	119.52	63.22
1990	18.23	116.63	61.65
2000	40.17	129.60	78.75
2004	32.89	123.59	77.17
2006	26.37	117.87	71.92
2010	25.42	127.79	72.67
2013	33.73	122.44	73.38
2015	28.96	121.16	73.66
2016	19.37	123.90	72.97
2017	26.72	121.40	72.15
2018	25.70	122.60	71.69
2019	21.63	102.16	68.19
2020	12.40	95.62	50.80
2021	24.12	99.69	58.57

Table 6: Barrier width standard deviation, barrier length, and vegetation cover for each available year at East Beach.

Year	Barrier Width Standard Deviation	Barrier Length (m)	Vegetation Cover (%)
1931	30.54	1044.45	30.27
1959	31.05	1049.82	43.65
1973	33.34	1044.46	44.15
1977	32.64	1049.05	39.31
1985	29.88	1062.15	29.88
1990	27.79	1054.24	0.00
2000	24.03	1047.73	39.53
2004	25.58	1050.37	34.49
2006	24.51	1063.95	37.75
2010	26.87	1055.84	50.08
2013	24.93	1063.91	82.12
2015	26.22	1061.56	78.32
2016	29.61	1048.34	84.10
2017	26.73	1041.85	52.60
2018	27.21	1042.59	52.78
2019	25.71	1061.09	62.19
2020	26.17	1081.13	13.70
2021	19.34	1075.43	34.97

Table 7: Annual maximum ice cover, back bay area, and median fetch distance for each available year at East Beach.

Year	Annual Max Lake Ice Cover (%)	Back Bay/ Lagoon Area (m²)	Median Fetch Distance (m)
1931		1486299.77	-
1959		1482629.85	-
1973	95.7	1485701.21	-
1974	88.5	-	-
1975	80.1	-	-
1976	95.4	-	-
1977	99.8	1493123.98	-
1978	100	-	-
1979	100	-	-
1980	93.4	-	-
1981	96	-	-
1982	99.1	-	-
1983	40.8	-	-
1984	95.7	-	-
1985	96	1485136.02	174795.83
1986	95.5	-	-
1987	88	-	-
1988	91.5	-	-
1989	91.6	-	-
1990	72.8	1462377.29	22941.81
1991	35.1	-	-
1992	89.8	-	-
1993	94.3	-	-
1994	96.7	-	-
1995	94	-	-
1996	100	-	-
1997	99.6	-	-
1998	5.4	-	-
1999	74.8	-	-
2000	90.7	1452330.42	64738.78
2001	94	-	-

2002	14.4	-	-
2003	95.7	-	-
2004	95.4	1453460.83	64738.78
2005	93	-	-
2006	21.9	1453019.01	64738.78
2007	95.8	-	-
2008	93.4	-	-
2009	95.5	-	-
2010	93.1	1452344.97	64738.78
2011	95.8	-	-
2012	13.9	-	-
2013	83.7	1450702.98	174795.83
2014	96.1	-	-
2015	98.1	1452798.52	64738.78
2016	78.7	1452492.21	174795.83
2017	35.5	1452366.50	174795.83
2018	95.1	1452316.07	174795.83
2019	94.3	1448459.31	174795.83
2020	15.9	1429350.59	64738.78
2021	85.7	1425697.86	-
2022	93.8	-	-

Table 8: Wind speed, wind direction based on the circular mean, wind direction based on fetch, and wave height for each available year at East Beach.

Year	Wind Speed (m/s)	Wind Direction (Circular Mean)	Wind Direction (Fetch)	Wave Height (m)
1985	4.19	176.29	93.54	0.44
1990	5.63	251.91	79.70	0.54
2000	5.47	168.13	96.99	0.46
2004	5.57	180.57	95.37	0.52
2006	5.55	195.58	96.29	0.48
2010	5.18	236.10	96.89	0.45
2013	5.06	200.87	96.23	0.38
2015	5.39	216.43	98.05	0.46
2016	5.12	205.17	94.15	0.43
2017	5.50	202.79	95.91	0.49
2018	5.51	179.24	94.28	0.51
2019	5.45	203.01	94.47	0.49
2020	5.91	220.33	101.55	0.53

Table 9: Nearshore slope of breached barrier beaches around the Great Lakes.

East Beach, Point Pelee National Park (Lake Erie)	0.01175
Hillman Beach, Hillman Marsh Conservation Area (Lake Erie)	0.01239
Conneaut Park, Conneaut, Ohio (Lake Erie)	0.00065
Elk Creek, Erie County, Pennsylvania (Lake Erie)	0.01143
Talbot Creek, Elgin County, Ontario (Lake Erie)	0.00909
Tyrconnell Beach, Tyrconnell, Ontario (Lake Erie)	0.00897
North Bar Lake, Empire Township, Michigan (Lake Michigan)	0.01992
Petobego Pond, Grand Traverse County, Michigan (Lake Michigan)	0.03513
Lakeside Park, Ajax, Ontario (Lake Ontario)	0.00988
Lynde Creek, Durham, GTA, Ontario (Lake Ontario)	0.01089
Petticoat Creek, Pickering, Ontario (Lake Ontario)	0.01155
Turtle/Sheridan Creek, Clarkson, Mississauga, Ontario (Lake Ontario)	0.01008
Wild Beach, Whitby, Ontario (Lake Ontario)	0.01034
Aquasabon River, Terrace Bay, Thunder Bay District, Ontario (Lake Superior)	0.04692
Lightfoot Bay, Skanee, Michigan (Lake Superior)	0.01825

Vita Auctoris

NAME: Jenny Gharib

PLACE OF BIRTH: Windsor, Ontario, Canada

YEAR OF BIRTH: 1998

EDUCATION: Holy Names High School, Windsor, Ontario
2012 – 2016

University of Windsor, Windsor, Ontario
2016 – 2020, B.ES.

University of Windsor, Windsor, Ontario
2020 – 2022, M.Sc.